Monthly Notices of the ROYAL ASTRONOMICAL SOCIETY

MNRAS **480,** 3376–3396 (2018) doi:10.1093/mnras/sty2041
Advance Access publication 2018 August 1

The frequency of dwarf galaxy multiples at low redshift in SDSS versus cosmological expectations

Gurtina Besla,[1]★ David R. Patton,[2] Sabrina Stierwalt,[3,4] Vicente Rodriguez-Gomez,[5] Ekta Patel,[1] Nitya J. Kallivayalil,[3] Kelsey E. Johnson,[3] Sarah Pearson,[6] George C. Privon[7] and Mary E. Putman[6]

[1]*Steward Observatory, University of Arizona, 933 North Cherry Avenue, Tucson, AZ 85721, USA*
[2]*Department of Physics & Astronomy, Trent University, 1600 West Bank Drive, Peterborough, Ontario, K9L 0G2, Canada*
[3]*Department of Astronomy, University of Virginia, 530 McCormick Road, Charlottesville, VA 22904, USA*
[4]*California Institute of Technology, 1200 East California Boulevard, Pasadena, CA 91125, USA*
[5]*Department of Physics and Astronomy, Johns Hopkins University, 3400 N. Charles Street, Baltimore, MD 21218, USA*
[6]*Department of Astronomy, Columbia University, Mail Code 5246, 550 West 120th Street, New York, NY 10027, USA*
[7]*Department of Astronomy, University of Florida, 211 Bryant Space Science Center, Gainesville, FL 32611, USA*

Accepted 2018 July 20. Received 2018 July 14; in original form 2018 April 23

ABSTRACT

We quantify the frequency of companions of low-redshift ($0.013 < z < 0.0252$) dwarf galaxies ($2 \times 10^8\,M_\odot < M_{star} < 5 \times 10^9\,M_\odot$) that are isolated from more massive galaxies in *SDSS* and compare against cosmological expectations using mock observations of the *Illustris* simulation. Dwarf multiples are defined as two or more dwarfs that have angular separations >55 arcsec, projected separations $r_p < 150$ kpc, and relative line-of-sight velocities $\Delta V_{LOS} < 150\,km\,s^{-1}$. While the mock catalogues predict a factor of two more isolated dwarfs than observed in *SDSS*, the mean number of observed companions per dwarf is $N_c \sim 0.04$, in good agreement with *Illustris* when accounting for *SDSS* sensitivity limits. Removing these limits in the mock catalogues predicts $N_c \sim 0.06$ for future surveys (LSST, DESI), which will be complete to $M_{star} = 2 \times 10^8\,M_\odot$. The 3D separations of mock dwarf multiples reveal a contamination fraction of ∼40 per cent in observations from projection effects. Most isolated multiples are pairs; triples are rare and it is cosmologically improbable that bound groups of dwarfs with more than three members exist within the parameter range probed in this study. We find that <1 per cent of LMC-analogues in the field have an SMC-analogue companion. The fraction of dwarf "Major Pairs" (stellar mass ratio >1:4) steadily increases with decreasing Primary stellar mass, whereas the cosmological "Major Merger rate" (per Gyr) has the opposite behaviour. We conclude that cosmological simulations can be reliably used to constrain the fraction of dwarf mergers across cosmic time.

Key words: galaxies: dwarf – galaxies: groups: general – Magellanic Clouds.

1 INTRODUCTION

Low-mass dwarf galaxies ($M_{star} < 5 \times 10^9\,M_\odot$) are the most common class of galaxy at all redshifts (Binggeli, Sandage & Tammann 1998; Karachentsev, Makarov & Kaisina 2013), and yet, their pair/group fractions have not been quantified observationally and compared to cosmological expectations in a consistent manner. In contrast, the interaction frequency between massive galaxies is actively studied, both observationally (e.g. Zepf & Koo 1989; Carlberg et al. 2000; Patton et al. 2002; Conselice et al. 2003; Bundy et al. 2004; Bell et al. 2006; Lin et al. 2008; Patton & Atfield 2008; Lotz et al. 2011; Man, Zirm & Toft 2016; Patton et al. 2016; Mundy et al. 2017; Ventou et al. 2017; Mantha et al. 2018, etc.) and theoretically (Blumenthal et al. 1984; Lacey & Cole 1993; Berrier et al. 2006; Maller et al. ; Guo & White 2008; Hopkins et al. 2010; Rodriguez-Gomez et al. 2015, etc.). Consequently, little is known about the frequency of dwarf–dwarf galaxy interactions and their role in the evolution of low-mass galaxies.

In this study, we quantify the fraction of dwarf galaxies with low-mass companions at low redshift utilizing both observational data from the Sloan Digital Sky Survey (*SDSS*) and "mock" galaxy catalogues created using the *Illustris-1* cosmological simulation, (Vogelsberger et al. 2014; Nelson et al. 2015). Our goal is to estab-

★ E-mail: gbesla@email.arizona.edu

© 2018 The Author(s)
Published by Oxford University Press on behalf of the Royal Astronomical Society

Downloaded from https://academic.oup.com/mnras/article-abstract/480/3/3376/5063581 by California Institute of Technology user on 28 November 2018

lish the reliability with which cosmological simulations can trace the hierarchical processes that are expected to influence the evolution of dwarf galaxies.

Environmental effects (the tidal field of a massive host, ram pressure stripping, etc.) are often presented as the dominant drivers of dwarf galaxy evolution. This is motivated by the fact that non-star forming, gas poor (quenched) dwarf galaxies are almost exclusively found in proximity to a massive host (Geha et al. 2012; Sánchez-Janssen et al. 2013; Bradford, Geha & Blanton 2015; Stierwalt et al. 2015). Satellite dwarf galaxies of the Local Group (van den Bergh et al. 2006; Grcevich & Putman 2009; Spekkens et al. 2014) and the Local Volume (Weisz et al. 2011) all exhibit similar distance-morphology relationships. Consequently, the role of mergers or interactions between dwarfs *prior* to their capture as a satellite of a massive galaxy has been largely ignored. However, this picture is rapidly changing.

While environmental processes are clearly needed to quench dwarf galaxies (e.g. Peng et al. 2010), they are not the only factors governing the evolution of low-mass galaxies. High-resolution dark matter simulations of Milky Way type haloes reveal that 10 per cent of surviving dwarf-mass satellites have experienced a major merger since $z = 1$ (Deason et al. 2015) and that 10 per cent of dwarfs host a satellite of at least 10 per cent its mass at $z = 0$ (Sales et al. 2013). Furthermore, 30–60per cent of all surviving dwarf satellites are expected to have been accreted as part of a low-mass group (Wetzel, Deason & Garrison-Kimmel 2015). Cosmologically, the tidal pre-processing of dwarf galaxies in low-mass multiples is not expected to be a rare phenomenon across cosmic time and presents an alternative pathway for galaxy evolution at the low-mass end. However, these theoretical predictions have yet to be tested systematically against observations.

We are only just starting to understand the impact of galactic pre-processing on the star formation histories (SFHs) and baryon cycle (supply and removal of gas) of dwarf galaxies. Earlier studies have suggested that many starbursting dwarf galaxies have companions (Noeske et al. 2001). Recently, the TiNy Titans (*TNT*) Survey studied the star formation rates (SFRs) and gas content of dwarf galaxy multiples (pairs and groups with stellar masses of 10^7 $M_\odot$ $< M_{\rm star} < 5 \times 10^9$ $M_\odot$) identified at low redshift ($0.005 < z < 0.07$) in *SDSS* (*TNT*; Stierwalt et al. 2015) and in the Local Volume ($<$ 30 Mpc, *TNT-LV*; Pearson et al. 2016). The *TNT* and *TNT-LV* surveys are designed to study the dwarf–dwarf merger sequence and its importance to the evolution of low-mass galaxies. This paper represents the theoretical counterpart to these studies.

The *TNT* surveys have provided mounting evidence that interactions between low-mass galaxies do impact the structure and SFHs of dwarf galaxies (e.g. Privon et al. 2017). In particular, Stierwalt et al. (2015) found that SFRs are elevated in dwarf pairs relative to their non-paired counterparts; dwarf–dwarf interactions appear to drive enhanced star formation. Furthermore, Pearson et al. (2016) illustrate that dwarf pairs in the Local Volume are often found with extended gaseous envelopes, compared to their non-paired counterparts, suggesting that the efficiency of gas removal can also be increased through dwarf–dwarf interactions. This is true for the Magellanic System, the closest example of a dwarf–dwarf interaction (Putman et al. 2003; Besla et al. 2010, 2012, 2013; Nidever et al. 2010; Diaz & Bekki 2011; Guglielmo, Lewis & Bland-Hawthorn 2014). Indeed, Marasco et al. (2016) use the EAGLE cosmological simulation (Schaye et al. 2015) to illustrate that satellite–satellite encounters may be more important than environmental effects (tidal/ram pressure stripping by the host) in the gaseous evolution of dwarf satellite galaxies.

With next generation photometric and spectroscopic instruments, such as LSST, DESI, WFIRST, etc., new detections of low-mass (or low-surface brightness) galaxies with companions are forthcoming. A glimpse of what lies ahead is highlighted by the recent discovery of seven isolated groups of dwarfs with 3–5 members in the *TNT* sample (Stierwalt et al. 2017). The newly discovered *TNT* groups provide us with a window into a process of hierarchical evolution that may have been much more common at high redshift. However, there is no existing framework to understand how these low-redshift groups fit in the prevailing cosmological model.

The average satellite mass functions of dwarf galaxies have been quantified in cosmological simulations (Dooley et al. 2017) and compared to observations in *SDSS* (Sales et al. 2013). Here, we expand such methods to create mock catalogues of cosmological dwarf multiples (pairs/groups) in isolated environments, accounting for the sensitivity limits of *SDSS* and line-of-sight properties (projected separation and relative velocities; including peculiar motions) that control the observational definition of companionship. Our goal is to assess whether or not the observed and theoretical fraction of dwarf multiples agree within the redshift and mass ranges where they can be reasonably compared: stellar masses between 2×10^8 $M_\odot$ $< M_{\rm star} < 5 \times 10^9$ $M_\odot$ at low redshift (Volume $\lesssim (100$ Mpc$)^3$; $0.013 < z < 0.0252$). Specifically, we aim to address the following questions:

(i) What is the observed fraction of dwarfs in a pair or group versus cosmological expectations?
(ii) What is the contamination fraction of dwarf multiples owing to projection effects?
(iii) What do cosmological simulations predict for the frequency of dwarf multiples in the era of deep photometric surveys like LSST?
(iv) What is the $z \sim 0$ fraction of dwarf "Major Pairs" (stellar mass ratio $>$1: 4)?
(v) What is the observed frequency of Magellanic Cloud analogues in the field versus cosmological expectations?
(vi) Are the recently discovered *TNT* dwarf groups (Stierwalt et al. 2017) consistent with cosmological expectations?

Through this analysis, we will establish the reliability of such simulations as probes of hierarchical processes at low masses at $z \sim 0$, lending credibility to their usage as predictors of the frequency of dwarf–dwarf interactions and mergers across cosmic time.

In Section 2, we describe our methodology to assign properties to galaxies (stellar mass, redshifts, isolation) and define survey volumes in both *SDSS* and *Illustris*. In Section 3, we quantify number counts of all galaxies (dwarfs and massive galaxies) and isolated dwarfs. Results for the frequency of dwarf multiples in *SDSS* and *Illustris* and predictions for next generation surveys are summarized in Section 4. We discuss the dwarf "Major Pair" fraction, the frequency of Magellanic Cloud analogues, and place the *TNT* groups of dwarfs in a cosmological context in Section 5. Finally, we conclude in Section 6.

2 GALAXY CATALOGUES

We define a "dwarf galaxy" as a galaxy with a stellar mass of 2×10^8 $M_\odot$ $< M_{\rm star} < 5 \times 10^9$ $M_\odot$. The upper mass limit corresponds to systems slightly more massive than the Large Magellanic Cloud (LMC; $M_{\rm star} = 3 \times 10^9$ $M_\odot$; van der Marel et al. 2002). According to the Tully–Fisher relation, this definition generally excludes galaxies with rotation curves that peak at 100 km s^{-1} or larger (Lelli, Fraternali & Verheijen 2014). For reference, the LMC's ro-

Downloaded from https://academic.oup.com/mnras/article-abstract/480/3/3376/5063581 by California Institute of Technology user on 28 November 2018

tation curve peaks at $\sim$90 km s^{-1} (van der Marel & Kallivayalil 2014).

The lower mass limit corresponds to the stellar mass of the Small Magellanic Cloud (SMC; $M_{\rm star} \sim 2 \times 10^8$ M$_\odot$; Stanimirovic, Staveley-Smith & Jones 2004; van der Marel, Kallivayalil & Besla 2009). The completeness of the SDSS catalogue drops rapidly with decreasing stellar mass as a function of redshift. Galaxies of stellar mass of $\sim 2 \times 10^8$ M$_\odot$ are the lowest mass galaxies that are complete in SDSS at the lowest redshift considered in this study ($z = 0.013$; see Section 2.4).

Galaxies with stellar masses larger than 5×10^9 M$_\odot$ are referred to as "Massive Galaxies". Dwarf multiples (pairs and groups) do not survive for very long as bound configurations about massive galaxies (e.g. Gonzalez & Padilla 2016). We thus require our dwarf galaxy sample to be sufficiently isolated from such systems, as described in Section 2.3.

In the following, we describe how stellar masses are defined for all galaxies in both the observational and cosmological data sets. Note that the cosmological galaxy samples will be referred to as "mock" galaxy catalogues.

2.1 Observational galaxy catalogue: *SDSS*

Following Stierwalt et al. (2015), our observational sample is drawn from the Legacy area of the *SDSS* Data Release 7 spectroscopic catalogue (Abazajian et al. 2009). We utilize only the continuous footprint, which covers 7296 deg^2 of the sky. Spectroscopic completeness of galaxies imaged is estimated at 88 per cent for galaxies with $14.5 < m_r < 17.5$ (Patton & Atfield 2008). Note that low-surface brightness galaxies and very close pairs will be preferentially missed. We apply lower limits on the anglar separation between dwarf galaxies ($r_p > 55$ arcsec; i.e. projected distances of 15–25kpc depending on the redshift) to avoid fibre collisions that can miss close pairs (Section 4.1).

We select galaxies from the *SDSS* value-added catalogue of Simard et al. (2011), which is a reprocessing of the *SDSS* photometry using bulge-disc decomposition and an improved handling of de-blending in crowded systems, such as close galaxy pairs. Stellar masses and associated errors are taken from Mendel et al. (2014, hereafter M14). We use the Sersic *ugriz* total stellar mass fits of M14, as recommended in their appendix B.2.1 (see also Patton et al. 2013).

We assume Gaussian errors and sample the M14 stellar mass errors randomly to generate 500 unique realizations of the entire stellar mass catalogue, each with a different set of stellar masses allowed within the errors. All statistics presented in this study are computed as the mean and standard deviation over these 500[1] realizations.

The M14 catalogue is restricted to galaxies with $14 < m_r < 17.77$, where m_r is the extinction-corrected r-band Petrosian magnitude from the *SDSS* data base. As such, we supplement the *SDSS* Massive Galaxy sample with bright galaxies ($m_r < 14$) identified in the NASA-Sloan Atlas (NSA) and adopt the associated stellar masses and redshifts quoted in the catalogue.[2] We do not randomly sample the stellar mass errors for the massive galaxy sample as we are not interested in the intrinsic properties of these galaxies.

[1]We have also repeated this study using 1000 unique realizations and found similar results within 1σ.
[2]http://www.nsatlas.org/data

Redshifts are adopted for dwarfs ($m_r > 14$) from the *SDSS* data release 9 (DR9) spectroscopic catalogue, which has an average redshift error of order 10^{-5}. In contrast, the average redshift error in DR7 is 10^{-3}, which is too large to meaningfully extract kinematic information for the dwarf multiples. The corresponding DR9 velocity errors are $\sim$4 km s^{-1}, computed at the average redshift of our sample ($z \sim 0.021$).

We assign redshifts to each galaxy in the sample in a similar fashion to the assignment of stellar mass: we assume Gaussian errors that are randomly sampled to generate the 500 unique realizations of the catalogue. As such redshift errors, although small, are accounted for in the determination of both the relative velocities and positions of dwarf multiples.

There is 98.9 per cent overlap between galaxies identified in the Simard et al. (2011) catalogues and those in DR9 (for $z < 0.05$). However, because we are using stellar masses from M14, who adopt DR7 redshifts, we further require that the difference between the DR7 and DR9 redshifts corresponds to a velocity difference less than 100 km s^{-1}. With this requirement, there is a $\sim$97.5 per cent overlap between the DR9 and M14 catalogues. The remaining $\sim$2.5 per cent of the sample are assigned DR7 redshifts and errors. A velocity error of 100 km s^{-1} corresponds to a stellar mass error of 0.06 dex at $z = 0.005$ and 0.01 dex at $z = 0.0252$. This is well below the average mass error in M14 of 0.1 dex. Moreover, the average redshift difference between our galaxy samples in DR7 and DR9 corresponds to a velocity difference of $\sim$15 km s^{-1}. This error is much lower than the velocity constraints that we later apply to define dwarf multiples ($\Delta V_{\rm LOS} = 150$ km s^{-1}; see Section 4.1).

2.2 Mock galaxy catalogue: *Illustris* & abundance matching

We utilize data from the *Illustris* Project (Vogelsberger et al. 2014): an N-body and hydrodynamic simulation spanning a cosmological volume of (106.5 Mpc)^3 to derive "mock" galaxy catalogues, which will be the basis for comparison to expectations from ΛCDM theory.

In this analysis, we use the highest resolution hydrodynamic *Illustris-1* (hereafter *Illustris Hydro*) version of the simulation suite, which simulates the growth of structure from $z = 127$ to $z = 0$. We have tested all of our results using the dark matter-only *Illustris-1-Dark* simulation, and find very good agreement (see Appendix A).

The *Illustris* Project adopts cosmological parameters consistent with WMAP-9 (Hinshaw et al. 2013): $\Omega_m = 0.2726$, $\Omega_b = 0.0456$, $\Omega_\Lambda = 0.7274$, $\sigma_8 = 0.809$, $n_s = 0.963$, and $h = 0.704$.

For this study, we will not use stellar masses that result from the explicit star formation prescription adopted in *Illustris Hydro*. There are large uncertainties in the star formation prescriptions appropriate for low-mass galaxies, which can strongly affect the evolution of low-mass systems. In particular, it has been found that stellar masses of dwarfs in *Illustris Hydro* are too high compared to observations (Genel et al. 2014). Different subgrid prescriptions for the physics of the interstellar medium are adopted by many teams and no consensus has yet been reached by the community. Instead, we derive all statistics using only the dark matter component of subhaloes identified in *Illustris Hydro*. We assign stellar masses via abundance matching utilizing the global baryonic fraction to convert the dark matter component to a total subhalo mass.

We utilize *Illustris Hydro* in this analysis because the growth of dark matter subhaloes is known to be affected by baryonic processes, such as feedback (e.g. Wetzel et al. 2016). As a result, many low-mass subhaloes that exist in *Illustris-Dark-1* can be destroyed at early times in *Illustris Hydro* (Chua et al. 2017).

Downloaded from https://academic.oup.com/mnras/article-abstract/480/3/3376/5063581 by California Institute of Technology user on 28 November 2018

Dark matter haloes and their associated substructures (or subhaloes) are identified in *Illustris Hydro* using the SUBFIND halo-finding routine (Springel et al. 2001; Dolag et al. 2009). Theoretical dwarf and massive galaxy analogue samples are then selected from the publicly available SUBFIND subhalo group catalogues generated at the $z = 0$ snapshot of the simulations. *Illustris Hydro* reaches a dark matter particle mass resolution of $m_{DM} = 6.3 \times 10^6$ $M_\odot$ per particle. We place a lower limit of $M_{DM} = 5 \times 10^9$ $M_\odot$, ensuring that all haloes are well-resolved into >790 particles. This mass is also roughly the dynamical mass of the SMC within 3 kpc (Harris & Zaritsky 2006).

2.2.1 *Assigning stellar mass to the mock galaxy catalogue*

We assume that the stellar mass associated with a given subhalo is a function of the maximum dark matter mass a subhalo has ever attained (see, e.g. Boylan-Kolchn, Besla & Hernquist 2011). Hydrodynamic cosmological simulations have supported this assertion, finding that halo mass grows in unison with stellar mass (Wellons & Torrey 2017). We utilize the abundance matching relations in Moster, Naab & White (2013) to assign a stellar mass to each subhalo, as outlined below.

We first identify the maximal dark matter mass ever achieved by each subhalo over its cosmic history ($M_{DM,\,max}$) using merger trees created with the recently developed SUBLINK code (Rodriguez-Gomez et al. 2015). Because we are searching for dwarf subhaloes in close proximity to each other, their dark matter distributions are likely truncated by tidal effects, making mass assignment via abundance matching less reliable if we choose their final descendent dark matter masses.

In addition, we require subhaloes to be separated by at least five times the gravitational softening length, which helps to assign reliable halo masses to merging systems. Similar methods have been applied to select Magellanic Cloud analogues in the Millennium-II simulation (Boylan-Kolchin et al. 2011).

A stellar mass is then assigned to a subhalo using the $z = 0$ Moster et al. (2013) relations (their equations 11–14), and the maximal total subhalo mass, $M_{subhalo} = M_{DM,\,max} \times \Omega_m/(\Omega_m - \Omega_b)$. To account for the scatter in the halo mass-stellar mass relation, we assume Gaussian errors using the 1σ errors for each parameter, as listed in table 1 of Moster et al. (2013), to randomly assign each subhalo a stellar mass. This procedure of assigning stellar mass is repeated every time we select a set of mock galaxies (see Section 2.4).

The resulting halo-stellar mass pairing will scatter about the mean abundance matching relation; see Fig. 1, where the dashed black line illustrates the mean relation from Moster et al. (2013). For a halo of mass 10^{11} $M_\odot$, abundance matching yields a mean stellar mass of $\log(M_{star}) = 9.0 \pm 0.3$. Uncertainties on stellar mass for the mock catalogue are thus roughly a factor 3–4 larger than those in the M14 catalogue.

Note that there are a number of cases in Fig. 1 where the derived stellar mass is larger than the scatter about the abundance matching relations at $z = 0$ (points to the far left). This is because $M_{DM,\,max}$, which was used to assign the stellar mass, is larger than $M_{DM,\,z=0}$. In each of these cases the dwarf subhalo has a companion dwarf in close proximity $r_p < 30$ kpc. However, in some cases the dwarf companion is at smaller angular separations than 55 arcsec and so we do not count it as part of a multiple (marked as grey points instead). Because the dwarf subhaloes are close together, their individual dark matter masses are ill-defined: either tides have stripped the outer halo, or the haloes overlap sufficiently that most of the mass is assigned to the companion, causing the dark matter mass to decrease substantially at $z = 0$ relative to their maximal halo mass. This is the reason the maximal halo mass is utilized to assign stellar mass.

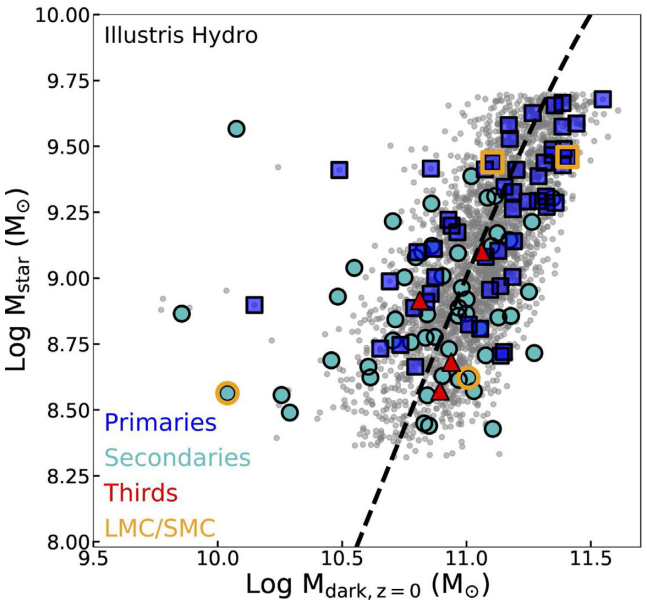

Figure 1. The stellar mass is plotted versus the descendent dark matter mass of each mock dwarf in the *Illustris Hydro* simulation at $z = 0$. All mock dwarfs are isolated from more massive galaxies (see Section 2.3). Gaussian errors are assumed using 1σ errors for each parameter in the Moster et al. (2013) relation to randomly assign a stellar mass to each subhalo, using the maximal mass the subhalo achieves. Isolated multiples (groups and pairs) are indicated by larger symbols, whereas companionless dwarfs are marked by grey points. Isolated analogues of the LMC+SMC pair (see Section 5.2) are marked by orange circles (SMC) and squares (LMC). The dashed black line indicates the mean abundance matching relation at $z = 0$ from Moster et al. (2013). Simulation data are presented for one representative sightline through the simulation volume. In practice this process is repeated for 500 different sightlines through the simulation volume, resampling the abundance matching relation errors each time (see Section 2.4).

2.2.2 *Assigning redshifts to the mock galaxy catalogue*

In this section, we describe how redshifts and line-of-sight velocities are assigned to our mock dwarfs. This methodology is complementary to the studies of Snyder et al. (2017) and Behroozi et al. (2015), who utilize the *Illustris* and *Bolshoi* simulations, respectively, to create mock galaxy catalogues and quantify the pair fraction of massive galaxies at higher redshift in comparison to observations.

Here, redshifts are assigned to mock dwarfs using the 3D distance and v_{los} of each subhalo in the simulation volume with respect to an observer placed randomly in the box. The redshift is computed as a combination of the redshift from the Hubble Flow, z_H, and the peculiar motion of the subhalo (v_{LOS}) along the observer's line of sight (red or blue shift). The observed redshift for the mock galaxy is thus

$$z = z_H + \frac{v_{LOS}}{c_{light}}, \quad (1)$$

where v_{LOS} can be positive or negative. z_H is determined by first computing the 3D distance of the mock galaxy to the observer (D_{LOS}). Then we assign the cosmological redshift using a look-up

Downloaded from https://academic.oup.com/mnras/article-abstract/480/3/3376/5063581 by California Institute of Technology user on 28 November 2018

table of comoving distances at a given redshift $D_C(z)$

$$D_C(z) = \frac{D_L(z)}{1+z}, \quad (2)$$

where $D_L(z)$ is the luminosity distance computed at a given redshift, z, using the *Illustris* cosmology. The cosmological redshift of the mock galaxy, z_H, is defined where $D_{\rm LOS} = D_C(z_H)$.

2.3 Selection of isolated dwarf galaxies

Low-mass galaxy groups are unlikely to survive as a bound configuration when in proximity to a massive galaxy (Gonzalez & Padilla 2016). The tidal field of the host can disrupt groups of dwarfs after even one pericentric passage. This explains the rarity of LMC+SMC binaries about Milky Way type hosts as determined by both observational (Liu et al. 2011; Robotham et al. 2012) and cosmological surveys (Boylan-Kolchin et al. 2011; Busha et al. 2011; Gonzalez, Kravtsov & Gnedin 2013) and by numerical simulations of the LMC+SMC binary evolution (Besla et al. 2012; Kallivayalil et al. 2013). There are indications that the number of dwarf galaxy pairs may be higher in the Local Group (Fattahi et al. 2010). However, the number density of dwarfs increases substantially in the presence of massive galaxies, increasing the likelihood of chance projections mimicking true multiples.

An isolation criterion also affords us the best comparison sample between the observations and simulation data as environmental effects can suppress star formation. This can cause extreme discrepancies between halo-stellar mass correlations and makes dwarfs redder in colour and thus harder to detect in surveys like the *SDSS*.

We define a dwarf galaxy to be isolated *if no Massive Galaxy ($M_{\rm star} > 5 \times 10^9$ M$_\odot$) can be identified that satisfies both of the following criteria*:

(i) A relative line-of-sight velocity $\Delta V_{\rm LOS} < 1000\,{\rm km\,s^{-1}}$. Patton et al. (2000) demonstrated that associations with massive galaxies at lower velocity separations are unlikely to be random.

(ii) Tidal Index, $\Theta > -11.5$. Following Karachentsev et al. (2013), we define the Tidal Index as

$$\Theta = \log\left(\frac{{\rm M_{star}}(10^{11}\,{\rm M_\odot})}{r_{\rm p}^3({\rm Mpc})^3}\right) - 10.97, \quad (3)$$

where $M_{\rm star}$ is the stellar mass of a given massive galaxy in units of 10^{11} M$_\odot$ and $r_{\rm p}$ is the projected separation between the Massive Galaxy and the dwarf (see also Karachentsev et al. 2004). Geha et al. (2012) find that quenched dwarf galaxies are not identified at separations larger than 1.5 Mpc from an L$*$ galaxy ($M_{\rm star} = 10^{11}$ M$_\odot$). This corresponds to $\Theta \sim -11.5$.

This isolation criteria is applied to both the observed and mock galaxy catalogues, as described below. The projected relative velocities ($\Delta V_{\rm LOS}$) between each dwarf and each Massive Galaxy are computed as

$$\Delta V_{\rm LOS} = c\frac{|z_{\rm d} - z_{\rm m}|}{1+z_{\rm avg}}, \quad (4)$$

where c is the speed of light, $z_{\rm d}$ is the redshift of the dwarf, $z_{\rm m}$ is the redshift of the Massive Galaxy, and $z_{\rm avg} = (z_{\rm d} + z_{\rm m})/2.0$.

Projected separations (r_p) are determined from the angular separation ($A_{\rm sep}$; in radians) between each dwarf and each Massive Galaxy and the angular diameter distance D_A:

$$r_p = A_{\rm sep} \times D_A \ {\rm kpc}. \quad (5)$$

To ensure that dwarf galaxies located at the *SDSS* survey boundaries are properly tested for isolation, the observational "Massive Galaxy" catalogue is supplemented with galaxies from the NSA catalogue that reside outside the *SDSS* continuous survey footprint. A dwarf galaxy is considered non-isolated and removed from the sample if at least one Massive Galaxy satisfies the above criteria. For each isolated dwarf, we record the Massive Galaxy with the largest Tidal Index that also satisfies $\Delta V_{\rm LOS} < 1000\,{\rm km\,s^{-1}}$. The stellar mass of these closest hosts and their projected separation to each isolated dwarf is plotted in Fig. 2 (SDSS results are on the left).

For the mock galaxy sample, the Isolation Criteria are applied as follows:

(i) Mock Massive Galaxies are identified within a physical cubic volume of (20 Mpc)^3 centred on each mock dwarf.

(ii) If this volume extends beyond the boundaries of the simulation, the periodic nature of the simulation is exploited to create a new (20 Mpc)^3 volume centred on the mock dwarf to ensure that dwarfs at the simulation boundaries can be properly tested for isolation.

(iii) The 3D position vector of each mock dwarf and Massive Galaxy from the observer location is translated into spherical coordinates, assuming the observer is located at coordinate (0,0,0) in a Cartesian system.

(iv) The angular separation between the mock dwarf and each mock Massive Galaxy in the (20 Mpc)^3 volume is computed and used to determine the projected separation as described above. This allows us to compute the Tidal Index Θ.

(v) Relative velocities are computed using mock redshifts that account for the peculiar motion of the mock galaxies along the line of sight (equation 4).

(vi) If any mock Massive Galaxy is found to satisfy both criteria, the mock dwarf is removed from the sample.

(vii) If no mock Massive Galaxies are found to satisfy both criteria, then the mock dwarf stays in the sample and the separation from the mock Massive Galaxy with the largest Tidal Index and $\Delta V_{\rm LOS} < 1000\,{\rm km\,s^{-1}}$ is recorded to double check that isolation is satisfied (see right-hand panel of Fig. 2).

This set of Isolation Criteria ensures that all dwarfs are more than 1.5 Mpc from an L$*$ type galaxy (Fig. 2; thick red dashed line). In practice, these criteria also ensure that none of our dwarfs have a Massive Galaxy within 500 kpc (Fig. 2; thin red dashed line).

2.4 Redshift limits and survey volume

We define the volume of our survey using redshift limits of $0.013 < z < 0.0252$. The survey volume is limited by: 1) the size of the *Illustris* volume of (106.5 Mpc)^3, which corresponds to a maximal redshift of $z = 0.0252$; 2) efforts to circumvent bias from cosmic variance; and 3) the sensitivity limits of *SDSS*, as explained below.

2.4.1 SDSS *sensitivity limits & catalogue volume*

The sensitivity limits of the *SDSS* catalogue are outlined in M14. The catalogue is not complete for dwarf galaxies in our redshift range (or for larger redshifts than considered here). The observability of dwarfs thus varies with redshift as a function of colour and stellar mass.

Downloaded from https://academic.oup.com/mnras/article-abstract/480/3/3376/5063581 by California Institute of Technology user on 28 November 2018

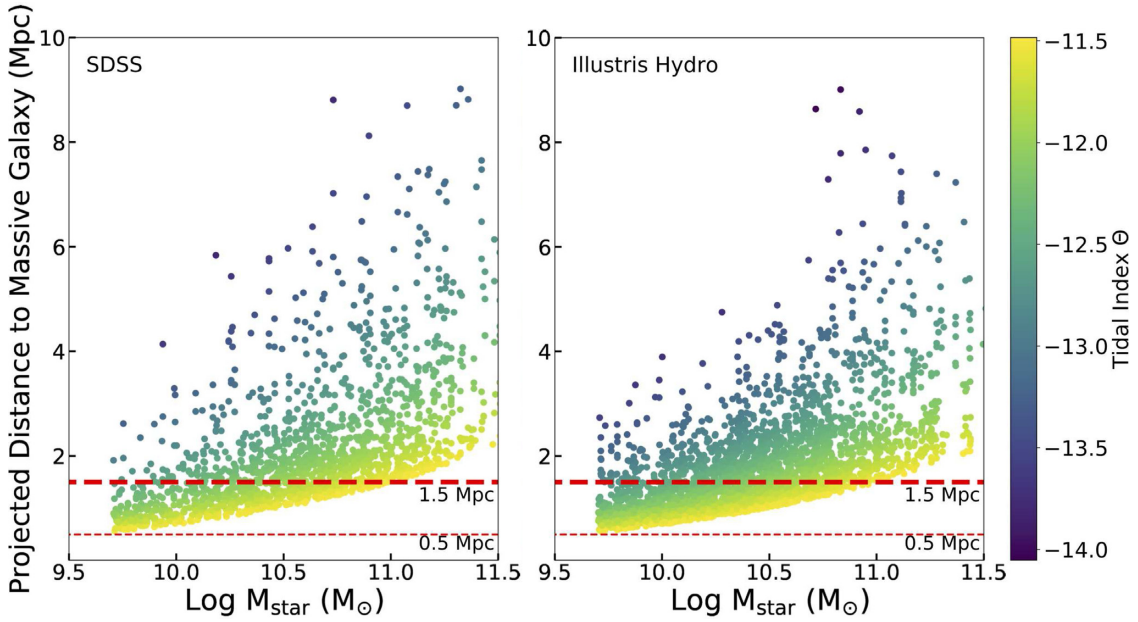

Figure 2. The stellar mass and separation of the Massive Galaxy ($M_{\rm star} > 5 \times 10^9$ M$_\odot$) with the largest Tidal Index (Θ, colour bar, equation 3) to each isolated dwarf identified in the *SDSS* (left) and *Illustris Hydro* (right) catalogues. Each Massive Galaxy is also required to have a relative velocity of $\Delta V_{\rm LOS} < 1000\,{\rm km\,s^{-1}}$ from each dwarf. All isolated dwarfs are found to be located more than 0.5 Mpc from all Massive Galaxies and more than 1.5 Mpc from all galaxies with $M_{\rm star} > 10^{11}$ M$_\odot$.

M14 define a fitting function that describes the minimum stellar mass observable for galaxies of a given colour at a given redshift

$$\log(M_{lim}/{\rm M}_\odot) = \alpha + \beta\log(z) + \gamma\log(1+z). \quad (6)$$

We adopt fitting parameters (α, β, γ)

$$\alpha = 12.36\,; \qquad \beta = 2.2\,; \qquad \gamma = 0.0. \quad (7)$$

These parameters correspond to the stellar mass completeness limit for all galaxies bluer than the green valley, as defined by M14. Note that because our sample is low redshift, we chose $\gamma = 0$ (versus $\gamma = 0.3932$ in Mendel et al. 2014) neglecting any redshift dependence in the fitting function.

These parameters best encompass our desired dwarf sample, which are expected to be blue or green in colour as galaxies with stellar masses between 10^8–10^9 M$_\odot$ are found to be typically gas rich and star forming in the field (Geha et al. 2006; Geha et al. 2012; Bradford et al. 2015). Furthermore, the average rest frame $g - r$ colour for the isolated *TNT* dwarf pairs in Stierwalt et al. (2015) is 0.267, with a maximum value of 0.557. In other words, all of the dwarf pairs found in *TNT* are either blue or green, but none are red.

In Fig. 3 (left) all dwarf galaxies in the M14 catalogue that satisfy our redshift and sensitivity limits are plotted as a function of mass and redshift. Points are colour-coded by the dwarf galaxy's restframe $g - r$ value. The black solid line illustrates the fitting function from equation (6). The sample drops off rapidly with redshift towards the low-mass end, but blue galaxies are observable over a larger mass range. The resulting average $g - r$ colour for the sample of isolated *SDSS* dwarfs we consider in this study is ∼0.41.

There are 28 dwarfs (14 pairs) in the Isolated *TNT* sample that are in the redshift range of our survey (blue circles in the left-hand panel of Fig. 3). However, given the adopted sensitivity limits, roughly 10 of the Isolated *TNT* sample (and only two pairs) in this redshift range overlap with our catalogue. Many *TNT* pairs are missed because the secondary falls below the observability limit. This means that by applying the listed sensitivity floor, we can only get a lower limit on the fraction of dwarf multiples. In Section 4.5, we remove these sensitivity limits but keep a mass floor of 2×10^8 M$_\odot$, which would recover 18 out of the 28 isolated *TNT* dwarfs (but only 8 out of 14 complete pairs).

The fact that the *TNT* pairs have members at masses below our sensitivity limits (black line in Fig. 3) strongly indicates that the dwarf multiple fraction determined in this study will significantly underestimate the true dwarf multiple fraction if the definition of "dwarf" were extended to lower masses. Our goal in this study is to compute the dwarf multiple fraction using parameters that can be reasonably reproduced by both observations and theory.

2.4.2 *Illustris simulation & mock catalogue volume*

To create the mock catalogue, sightlines are drawn through the *Illustris* simulation volume starting from a random location in the full (106.5 Mpc)^3 simulation volume and using a random viewing perspective. Because the simulation boundary conditions are periodic, the full volume can be recreated regardless of the chosen starting location or viewing orientation. Note we could exploit the periodic boundary conditions to expand the volume to larger redshifts (e.g. Snyder et al. 2017). However, the sensitivity limits of *SDSS* at larger redshift (Fig. 3) imply that the dwarf statistics would not increase appreciably.

As indicated in Fig. 4, an 'observer' is placed at a randomly selected starting location with a randomly chosen viewing direction. The 3D distance is computed between the observer and each subhalo as well as the velocity of each subhalo along the line of sight to the observer ($v_{\rm los}$).

Only those subhaloes with redshifts within the specified redshift limits are included in the analysis. This process is repeated 500 times, adopting a new observer location and viewing perspective each time (e.g. Schematic B in Fig. 4). All statistics presented

Downloaded from https://academic.oup.com/mnras/article-abstract/480/3/3376/5063581 by California Institute of Technology user on 28 November 2018

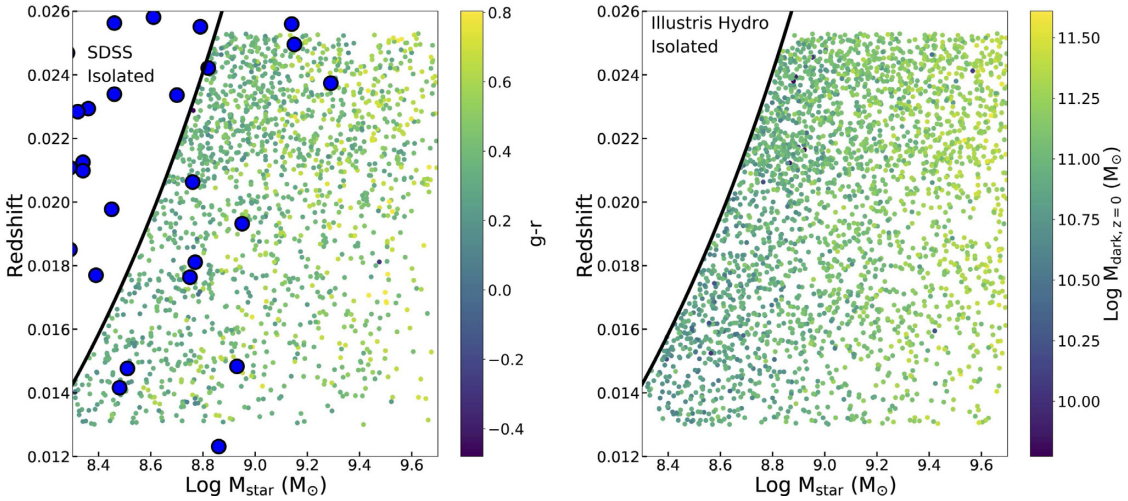

Figure 3. Redshift versus stellar mass of isolated *SDSS* dwarfs (*Left*) and mock dwarfs (*Right*) that satisfy the redshift and stellar mass limits adopted in this study. The black solid curve illustrates the adopted sensitivity limits as a function of stellar mass (equation 6). All dwarfs plotted here are isolated from more massive galaxies, as defined by the isolation criteria outlined in Section 2.3. *Left:* Dwarfs are colour-coded by rest frame $g - r$ colour. Blue galaxies are defined as having: $g - r < 0.4$, Green: $0.4 < g - r < 0.6$ and Red: $g - r > 0.6$. On average, the *SDSS* dwarfs have $g - r \sim 0.41$. Only 10 of the 28 *TNT* dwarfs (larger blue circles) would be included in our catalogue, and only two pairs out of 14 (the primaries are typically selected, but the secondaries fall below the sensitivity limit). *Right:* Results are plotted for one realization of the *Illustris Hydro* catalogue. Points are colour coded by the descendent ($z = 0$) halo mass of the mock dwarf. Note that more isolated dwarfs are identified in the mock catalogues than in *SDSS*; see Table 2.

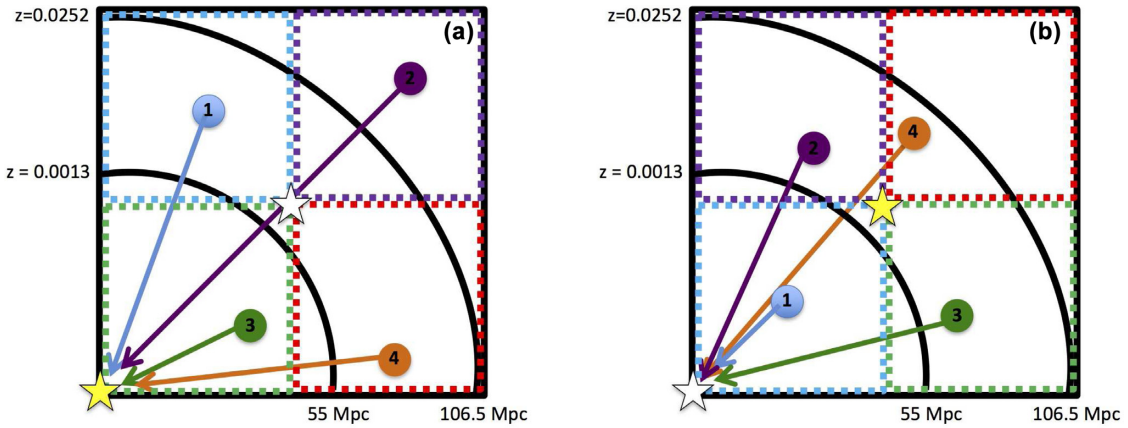

Figure 4. Schematic illustrating how the simulation volume is sampled to generate 'mock' galaxy catalogues. Schematic A (left) illustrates a 2D view of the simulation volume for one viewing perspective, where the observer is placed at the bottom left (coordinate 0,0; yellow star). For example subhaloes are marked by coloured circles, with line-of-sight vectors drawn to the observer. Black arcs indicate the redshift limits defined for the catalogue ($0.013 < z < 0.0252$). In Schematic A, only subhaloes 1 and 4 (blue and orange) would be included in this realization of the mock survey volume. Schematic B (right), represents a different realization of the same volume, where both the observer location and viewing perspective have been changed relative to Schematic A. To generate Schematic B, the observer is moved to the centre of Schematic A (white star) and we choose a different viewing perspective (the +y-axis in Schematic B is the -x-axis in Schematic A). The volume is then recreated, with the white star now at coordinate (0,0). Coloured dashed boxes are included to mark how the volume has been re-ordered from Schematic A to B. Given that the simulation boundary conditions are periodic, the volume can be reshuffled self-consistently – in the new realization of the volume, the observer in A (yellow star, at 0,0) is now at the centre of volume B. The survey redshift limits are redrawn (black arcs) and new redshifts are defined in volume B for each subhalo. The new survey volume in Schematic B thus encompasses different regions of the simulation volume than that of Schematic A. In particular, now subhaloes 2, 3, and 4 are included in the catalogue (purple, orange, and green). This process is repeated 500 times to generate the statistics quoted in this study.

in this study for the 'mock' galaxy catalogues are averaged over the 500 different realizations of the survey volume.

We have adopted a lower redshift limit of $z > 0.013$, which corresponds to a comoving distance of ∼55 Mpc. This was chosen so that only ∼half of the entire simulation volume is utilized for the selection of galaxies for a given combination of observer location and viewing perspective. As a result, we can sample a different volume each time the mock galaxy catalogue is generated. This allows us to address biases in our statistics introduced by cosmic variance and sampling bias. We are sampling different survey volumes that are affected by different large-scale structures, rather than sampling the same volume repeatedly.

With redshift limits of $0.013 < z < 0.0252$ the corresponding volume for our observational sample in *SDSS* is ∼(95 Mpc)^3. For the *Illustris* simulations, this redshift range corresponds to a volume of ∼(81 Mpc)^3, a factor of ∼1.4 times smaller than the observational

Downloaded from https://academic.oup.com/mnras/article-abstract/480/3/3376/5063581 by California Institute of Technology user on 28 November 2018

volume and a factor of ∼2 smaller than the total simulation volume. In other words, the adopted mock survey volume covers 1/8th of the sky (0.5π steradians), while *SDSS* covered ∼18 per cent of the sky, which yields a ratio of ∼1.4. This survey volume is significantly smaller than that sampled by the *TNT* survey ($0.005 < z < 0.07$; Stierwalt et al. 2015), but affords us the fairest comparison between the *SDSS* catalogue and the *Illustris* simulation volume.

The mock catalogue generation includes peculiar motions when determining the redshift and is thus consistent with the measurement of observational redshifts, as it is the sum of the Hubble flow and the peculiar velocity. Note that peculiar motions may cause us to assign companions to dwarfs that are actually at much larger 3D separations. This should affect both the mock and observed galaxy catalogues (see Section 4.1).

At this point, the mock galaxy sample is complete at all stellar masses within the mock survey volume. However, as described in the previous section, *SDSS* sensitivity limits imply a strongly increasing incompleteness as a function of increasing redshift and decreasing stellar mass (Fig. 3; left). To ensure the mock and observed dwarf galaxy catalogues are comparable, we apply the same sensitivity limits, as a function of redshift and stellar mass, to both the observed and mock galaxy catalogues, as described by equation (6). As a result, the mock catalogues will be similarly incomplete as a function of stellar mass (see right-hand panel of Fig. 3).

3 RESULTS: GALAXY COUNTS WITHIN THE OBSERVATIONAL AND MOCK SURVEY VOLUMES

3.1 Total galaxy counts: massive galaxies & dwarfs

Baryonic effects (stellar feedback, reionization) can dramatically affect galaxy counts at the low-mass end (Kravtsov 2010; Cui et al. 2012; Sawala et al. 2013; Chua et al. 2017). Here we compare galaxy counts within our survey volume ($0.013 < z < 0.0252$) for massive galaxies ($M_{\rm star} > 5 \times 10^9$ M$_\odot$) to ensure the observational and 'mock' galaxy catalogues yield consistent results in a mass regime where baryonic effects should not play a significant role (i.e. a mass regime where the stellar halo mass relations are well calibrated Genel et al. 2014). We then extend this analysis to the dwarf galaxy regime.

For the 'mock' galaxy catalogues, we quote statistics averaged over 500 sightlines that randomly sample the *Illustris Hydro* simulation volume, as described in the previous section and by Fig. 4. For the *SDSS* dwarf galaxy counts, we have randomly sampled the stellar mass and redshift error space assuming Gaussian errors from M14 and *SDSS* DR9, respectively, to generate 500 versions of the dwarf galaxy catalogue. Galaxy counts are computed as the mean over these catalogue realizations and the quoted errors are the standard deviations. Results are summarized in Table 1.

Note that we have not generated multiple versions of the massive galaxy catalogue ($M_{\rm star} > 5 \times 10^9$ M$_\odot$) as the *SDSS* DR9 survey is complete with respect to stellar mass for such galaxies over the redshift range considered. Given the small standard deviation in dwarf galaxy counts, this omission is not expected to significantly affect the galaxy counts of massive galaxies listed here. Also, as described in Section 2.1, we supplement the observed catalogue with massive galaxies identified in the NSA catalogue.

From Table 1, the number densities for Massive Galaxies are consistent between observations and theory, as expected as the feedback prescriptions adopted in *Illustris* are calibrated such that the stellar halo mass relation agrees with the observed number counts of Massive Galaxies (Vogelsberger et al. 2014). The difference in the total number counts reflects the factor of 1.4 larger volume of the *SDSS* footprint versus the *Illustris* volume.

The dwarf number densities are more discrepant, but still agree within 2σ. On average there appear to be more mock dwarfs than in *SDSS*, which is likely a manifestation of the missing satellite problem. Many of these dwarf subhaloes are in proximity to a massive host, and would likely be quenched by environmental processes, and therefore unobservable at low masses given our optimistic cuts in colour for the observability of dwarfs in *SDSS* (see Fig. 3). In the next section, we apply an isolation criterion to identify dwarfs that would still be star forming and thus bluer in colour in order to provide a fair comparison between the observations and the simulation data.

3.2 Isolated dwarf galaxy counts

In this section, the properties (number counts, mass distributions) of mock and observed dwarfs that are isolated from Massive Galaxies are quantified and compared for consistency. Recall, the distribution of isolated *SDSS* dwarfs are plotted as a function of redshift in the left-hand panel of Fig. 3, with mock catalogue results on the right.

Properties of the isolated dwarfs are summarized in Table 2. As expected, the number density of isolated dwarfs is much lower than that of non-isolated dwarfs in the observed and both mock galaxy samples (factor of 3 and 2, respectively). However, the mean number density of dwarfs in the mock catalogue is still a factor of 2 larger than that observed in *SDSS*. Note that the results do still agree within 2σ and the minimum density of mock isolated dwarfs identified across all 500 realizations of the *Illustris* volume is 0.003 $(\rm Mpc)^{-3}$, in agreement with the observed value. Despite the higher number density of dwarfs in the mock catalogues the mean stellar mass of isolated dwarfs is consistent with observations; all catalogues yield $<\log(M_{\rm star}/{\rm M}_\odot)> = 9.1 \pm 0.3$.

On average, there is a factor of ∼2 more mock dwarfs than observed in *SDSS* in a given volume (Table 2). There are a number of possible explanations for this discrepancy, e.g.:

(i) There are more low-surface brightness dwarf galaxies for the same stellar mass that are not currently observable given the sensitivity of *SDSS* (Blanton et al. 2005; Klypin et al. 2015). Their detection might be possible with new observing strategies (Greco et al. 2017; Danieli, van Dokkum & Conroy 2018) or when surveys like *LSST* come online.

(ii) Environmental effects are not the only explanation for the subhalo overabundance problem. Wetzel et al. (2016) have shown that different choices in star formation and feedback prescriptions can help remedy the problem. We do not explicitly account for the stellar mass formed in the simulation and thus do not account for this effect. However, while we are only exploring a factor of 10 in mass, it is not clear that such processes would similarly affect mass growth across this dwarf mass regime (Di Cintio et al. 2014).

(iii) Reionization may hinder early stellar mass growth, reducing the number of observable low-mass galaxies across the mass range probed (e.g. Wyithe & Loeb 2006). However, it is unclear how well this would work at LMC mass ranges.

(iv) There are fewer massive hosts at cluster mass scales ($M_{\rm star} \sim 10^{12}$ M$_\odot$) in the *Illustris* volume than in our selected *SDSS* volume (which is 1.4 times larger). In fact there are no systems at this stellar mass scale in our mock Massive Galaxy catalogues, but there are three in our *SDSS* Massive Galaxy Catalog. The Isolation

Downloaded from https://academic.oup.com/mnras/article-abstract/480/3/3376/5063581 by California Institute of Technology user on 28 November 2018

Table 1. Dwarf and Massive Galaxies in the *SDSS* and mock survey volumes. All values are the mean number counts and standard deviations computed over 500 realizations of the respective catalogues. *Columns 2 and 4) SDSS* values account for a spectroscopic completeness of 88%. Note that the stellar masses for the *SDSS* massive galaxies are not randomly sampled, and so the number count and density are listed without uncertainties. *Columns 3 and 5)* $n_{\rm massive}$ and $n_{\rm dwarf}$ refer to the number density of Massive and dwarf galaxies, respectively.

Catalogue	# Massive Galaxies	$n_{\rm massive}$ (Mpc)$^{-3}$	# Dwarf Galaxies	$n_{\rm dwarf}$ (Mpc)$^{-3}$	Volume (Mpc)^3
SDSS	6944	0.010	7860 ± 35	0.010	7.78×10^5
Illustris Hydro	4810± 741	0.009 ± 0.001	9165 ± 1607	0.017 ± 0.003	5.50×10^5

Table 2. Number of dwarf galaxies in the observed and mock survey volume that are isolated from all massive galaxies ($M_{\rm star} > 5 \times 10^9$ M$_\odot$). All values are the mean and standard deviation computed using 500 realizations of the respective catalogue. *Columns 2 and 3) SDSS* DR9 observed counts are listed accounting for a spectroscopic completeness of 88%. *Column 3)* $n_{\rm dwarfiso}$ refers to the number density of isolated dwarfs in the survey volume, following criteria listed in Section 2.3.

Catalogue	# Isolated Dwarfs	$n_{\rm dwarfiso}$ (Mpc)$^{-3}$
SDSS	1,909 ± 15	0.00245 ± 0.00002
Illustris Hydro	2,829 ± 422	0.0051 ± 0.0008

Criteria will thus remove more dwarfs in the observed catalogue than in the mock catalogue.

These four possibilities may be testable in next generation versions of cosmological simulations – particularly ones with larger volumes and different baryonic physics (e.g. Illustris-TNG, Springel et al. 2017). It remains a challenge to explain how these processes would uniformly affect the number density across the mass range probed in this study.

In Fig. 5, the fraction of mock and observed isolated dwarf galaxies is plotted for five equally spaced mass bins. Thus, although the total number of dwarf galaxies in the mock catalogues is higher than observed, the fraction of dwarfs per mass bin shows very good agreement. Since we are concerned with the ratio of dwarfs with companions relative to the total dwarf population, we expect that such ratios will be physically meaningful.

If the solution to the discrepancy between theory and observations is missing low-surface brightness galaxies, Fig. 5 suggests, perhaps surprisingly, that a similar fraction of low-surface brightness dwarfs are missing across all mass bins.

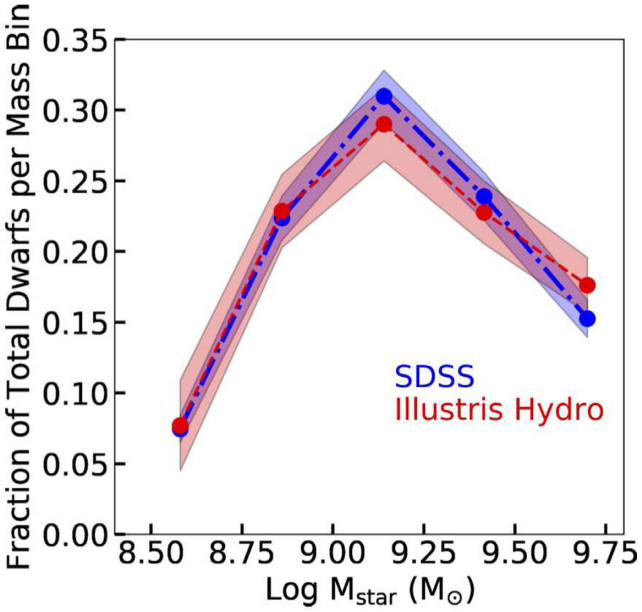

Figure 5. Number of isolated dwarf galaxies per stellar mass bin, normalized by the total number of dwarf galaxies in the entire respective catalogue. Five mass bins are equally spaced in log ($M_{\rm star}$) intervals of 0.28 starting at 8.3 to 9.7. Circles mark the end of each mass bin and the mean value of the ratio. Shaded regions indicate 2σ errors. The *SDSS* results are denoted by the blue dash–dotted line. *Illustris Hydro* results are plotted in red (dashed), showing good agreement. The rapid decline in all catalogues at low masses is a result of the sensitivity limits (equation 6).

4 RESULTS: FREQUENCY OF DWARF MULTIPLES AND PREDICTIONS FOR NEXT GENERATION SURVEYS

In the following sections, we quantify the frequency of isolated dwarf multiples, where all galaxy members have stellar masses from 2×10^8 M$_\odot$ $< M_{\rm star} < 5 \times 10^9$ M$_\odot$ and none are in proximity to a Massive Galaxy ($M_{\rm star} > 5 \times 10^9$ M$_\odot$).

In Section 4.1, we define our selection criteria for dwarf multiples. In Section 4.2, the mean number of companions per dwarf galaxy (N_c) is computed for all catalogues and calibrated for projection effects (multiples with 3D separations less than 300 kpc) using the cosmological catalogues. This is further quantified as a function of dwarf mass, $N_{c,m}$ in Section 4.3. In Section 4.4, we compute the frequency of dwarf pairs versus triples or higher order multiples for dwarf galaxies in the adopted mass range. Finally, in Section 4.5, we calibrate the *SDSS* results for completeness using the mock catalogues in order to make predictions for future surveys that will be complete to stellar masses as low as 2×10^8 M$_\odot$ out to 100 Mpc.

4.1 Identification of isolated dwarf multiples

We seek to identify dwarf galaxies with close companions that have separations and relative velocities that are plausible for tidally interacting, bound systems of this mass scale. Informed by results from the *TNT* surveys and numerical simulations of the Magellanic Clouds, dwarfs are deemed associated if they have a relative line-of-sight velocity less than 150 km s^{-1}, angular separation <55 arcsec, and a projected separation r_p <150 kpc. *SDSS* fibre collisions reduce the number of detectable companions at angular separations <55 arcsec, which corresponds to projected separations of ∼15–25kpc over the redshift range probed in this study.

In *Illustris*, the gravitational forces exerted by dark matter particles are softened on a comoving scale of $\epsilon = 1.4$ kpc. We are thus unable to resolve subhaloes that are separated by less than roughly five softening lengths, corresponding to a separation of roughly 11 kpc at $z = 0$. In practice, there are very few dwarf pairs that are identified with physical separations less than 15 kpc – this is likely

Downloaded from https://academic.oup.com/mnras/article-abstract/480/3/3376/5063581 by California Institute of Technology user on 28 November 2018

due to SUBFIND's inability to distinguish haloes separated by such small distances (see, e.g. Rodriguez-Gomez et al. 2015). Since the projected separation is always smaller than the 3D separation, by applying a limit of 55 arcsec on the angular separation, we ensure 3D separations large enough to avoid this issue.

The projected separation upper limit is roughly R_{200} for the most massive dwarf subhaloes in the mock catalogue ($M_{\rm dark} \sim M_{200} \sim 4.0 \times 10^{11}$ M$_\odot$; see Fig. 1). Furthermore, Stierwalt et al. (2015) found that SFRs in dwarf galaxy pairs are elevated relative to non-paired dwarfs even at separations of 120 kpc. An upper limit of 150 kpc will thus ensure that all plausibly interacting dwarfs are identified.

The upper limit on the line-of-sight velocity corresponds to the escape speed of our most massive dwarfs at a distance of 150 kpc. The selection criteria thus ensures that bound dwarf pairs will be captured even at large separations. For reference, the 3D velocity difference between the Magellanic Clouds is $\sim$130 km s^{-1} (Kallivayalil et al. 2013) and their 3D separation is $\sim$23 kpc; our criteria would allow for the selection of such analogues.

Note that these criteria differ from those adopted by the *TNT* survey (Stierwalt et al. 2015), where dwarf pairs were selected to have separations less than 50 kpc and relative velocities less than 300 km s^{-1} (although the majority of the sample have velocities less than 150 km s^{-1}). We adopt a larger separation limit because of the issues with close separations outlined above. We also adopt a lower relative velocity limit in order to minimize the frequency of chance projections.

4.1.1 *Selection of* physical *and* projected *dwarf multiples*

Using the defined *SDSS* and mock, isolated dwarf galaxy catalogues, "*Projected*" dwarf multiples are identified using the following steps based on their projected separations and relative line-of-sight velocities.

(i) All isolated dwarf galaxies are rank-ordered by stellar mass.

(ii) Starting with the most massive dwarf, the projected separation and line-of-sight velocity difference are computed between that dwarf and every other dwarf in the isolated catalogues.

(iii) All other dwarf galaxies located with angular separations <55 arcsec, projected separations of $r_p < 150$ kpc, and $\Delta V_{\rm LOS} < 150$ km s^{-1} of the given dwarf are stored as companions. The angular separation limit is applied to all catalogues to avoid incompleteness owing to fibre collisions in *SDSS* and create a similarly constrained mock catalogue.

(iv) The above steps are repeated for the next most massive dwarf.

All steps are repeated for 500 realizations of the *SDSS* and *Illustris Hydro* catalogues. The resulting catalogue of multiples will be referred to as *"SDSS"* and *"Illustris Hydro Projected"* in subsequent plots.

In Section 3.2, it was shown that the number density of isolated mock dwarfs is roughly a factor of two larger than that observed (Table 2). While the relative fraction of isolated dwarfs is consistent between theory and observations (Fig. 5), it is possible that the higher density of dwarfs will result in a larger frequency of dwarf multiples if they are selected based on projected properties alone.

To address this issue, we consider a second method for identifying mock dwarf multiples with small 3D separations. Before step 2 in the methodology outlined above, an additional step is introduced. Starting with the most massive dwarf, we first identify all isolated mock dwarf galaxies located within a 3D sphere 300 kpc in radius centred on the target mock dwarf and then proceed to step 3. This ensures that the contamination fraction from projection effects will be minimized. In contrast, the *Illustris Hydro Projected* sample may contain mock dwarfs separated by much larger 3D distances that appear to be in close proximity owing to projection effects. This process is repeated for 500 realizations of the dwarf mock catalogue to create a sample that will be referred to as *"Illustris Hydro Physical"* in subsequent plots.

Examples of the resulting distribution of dwarf multiples for the three catalogues (*SDSS, Illustris Hydro Projected, Illustris Hydro Projected*) are plotted in Fig. 6.

This figure illustrates the projected separation between each member of the multiple and the primary (most massive) dwarf galaxy member (excluding the primary itself). Results are plotted for one representative realization of each catalogue. The solid line indicates the observational limitations in resolving close pairs owing to *SDSS* fibre collisions. Since we have enforced a minimum angular separations of 55 arcsec, no multiples lie to the left of the solid line. When a 3D separation of 300 kpc is enforced (*Physical* criteria; right-hand panel in Fig. 6), most triples at wide separations are no longer identified. In contrast, multiples with separation less than 50 kpc are found to be robust against projection effects. The *TNT* dwarf pairs were all chosen to have separations less than 50 kpc; this study indicates that the *TNT* dwarf pairs are likely to be true pairs.

By repeating this process over multiple realizations of each catalogue, we will compute average statistics for the frequency of dwarf multiples, the number of members, stellar mass distributions, and kinematic properties.

4.2 Mean number of companions per dwarf galaxy (N_c)

Following Patton et al. (2000), we define N_c as the mean number of companions per galaxy. N_c is the total number of isolated dwarf companions (i.e. the sum of all pairs, triples, etc., that satisfy the criteria for multiples defined in Section 4.1), divided by the total number of isolated dwarf galaxies in each catalogue.

N_c is computed for all isolated dwarf galaxy multiples in each realization of the *SDSS* and mock catalogues (*Illustris Hydro Projected* and *Illustris Hydro Physical*). The results are then averaged over all 500 realizations of each catalogue. The resulting mean N_c and standard deviation for each catalogue are summarized in Table 3.

Agreement is best seen between the *SDSS* and *Illustris Hydro Projected* catalogues (agreement is within 1σ). In Section 2.3, concerns were raised that because the number density of mock dwarfs is too high relative to observations, the frequency of mock projected pairs would also be too high. However, we have shown here that the fraction of multiples is not overproduced, just as the fraction of dwarfs per mass bin is also in agreement between observations and theory (Fig. 5).

When the *Physical* selection criteria are applied to the mock catalogue, Table 3 and Fig. 7 illustrate that the average N_c decreases by $\sim$40 per cent. In other words, $\sim$40 per cent of *SDSS* multiples may have 3D separations larger than 300 kpc, despite their apparent proximity in projection. McConnachie, Ellison & Patton (2008) find a similar contamination fraction when identifying massive, compact galaxy groups in the Millennium simulation. This contamination fraction is also consistent with the study of Wilcots & Prescott (2004), who found that a significant fraction of nearby dwarf galaxies with a projected dwarf companion (such as in the

Downloaded from https://academic.oup.com/mnras/article-abstract/480/3/3376/5063581 by California Institute of Technology user on 28 November 2018

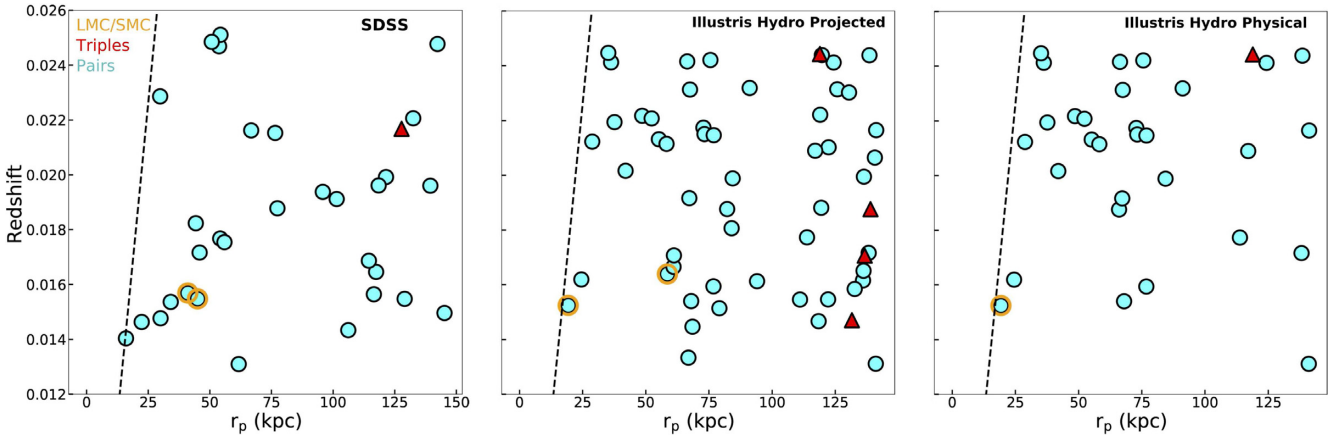

Figure 6. The projected separation between the primary of a dwarf multiple (i.e. most massive dwarf) and the second (cyan circles) or third (red triangles) member is plotted versus the average redshift of the primary-secondary or primary-third combination. Unique multiples are plotted for one representative realization of the *SDSS* (left) and mock catalogues, *Illustris Hydro Projected* (centre) and *Illustris Hydro Physical* (right). The dashed black line indicates an angular separation of 55 arcsec at each redshift. All dwarf companions are required to have separations from the primary that are larger than this value at a given redshift. LMC-SMC analogues are marked by orange circles (see Section 5.2). Dwarf triples identified at large projected separations (r_p >100 kpc) are found to have 3D separations greater than 300 kpc, failing the *Physical* criteria (two red triangles in middle panel, versus one in right-hand panel). The identification of multiples with small projected separation, like Magellanic Cloud analogues (r_p < 100 kpc) and the *TNT* sample (r_p < 50 kpc), appears robust against projection effects.

Table 3. N_c: Mean Number of Dwarf Companions per Dwarf *Column 2)* Method for defining multiples (see Section 4.1.1). *Column 3)* The mean N_c and standard deviation computed by averaging over 500 realizations of each catalogue. *The Last Row* indicates the expected mean fractional number of *Physical* companions in the *SDSS* sample. The *SDSS* N_c is corrected for contaminants owing to projection effects using the fractional difference between the *Physical* and *Projected* results of the *Illustris Hydro* mock galaxy catalogue.

Catalogue	Method	N_c
SDSS	Projected	0.039 ± 0.003
Illustris Hydro	Projected	0.034 ± 0.005
Illustris Hydro	Physical	0.021 ± 0.003
SDSS-Correction	Physical	∼0.024

sample of Odewahn 1994) show no strong signs of tidal disturbance in their outer HI structure.

We utilize the theoretical contamination fraction to calibrate the *SDSS* N_c for projection effects (see also Patton & Atfield 2008), resulting in the prediction that $N_c = 0.024$ for the mean number of companions per dwarf with physical separations less than 300 kpc (see Table 3).

4.3 Mean number of companions per dwarf per mass bin ($N_{c,m}$)

Fig. 7 illustrates the mean number of companions per dwarf per stellar mass bin, $N_{c,m}$ (i.e. N_c per stellar mass bin).

$N_{c,m}$ computed for the *SDSS* catalogue (blue) decreases from the lowest mass bin towards higher masses. The mock catalogues show qualitatively the same behaviour, with the best agreement with *SDSS* seen in *Illustris Hydro Projected*.

Note that the higher fraction of companions indicated by the *SDSS* sample in the lowest mass bin may be a result of sensitivity limits being biased towards blue colours. Indeed, there are only ∼130 dwarfs in the *SDSS* sample in the lowest mass bin of Fig. 7. Stierwalt et al. (2015) showed that dwarfs in pairs have higher SFRs,

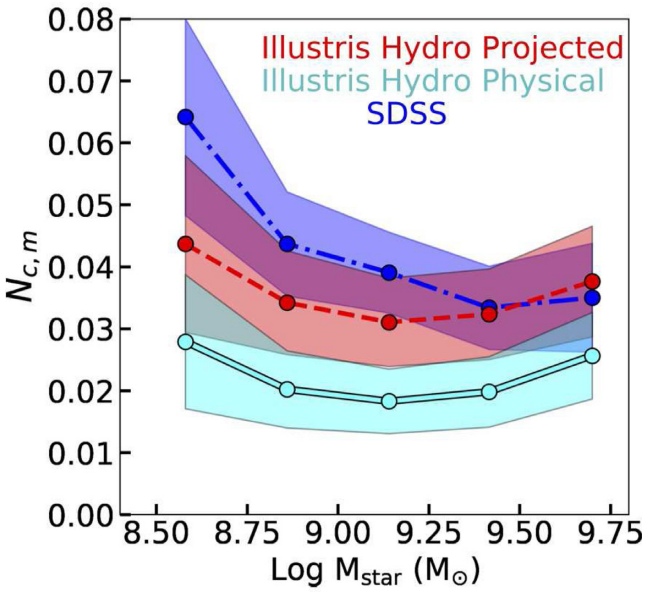

Figure 7. The mean number of companions is plotted per stellar mass bin, $N_{c,m}$. This represents the number of dwarf companions (of any mass within the defined dwarf mass range) per dwarf in the listed stellar mass bin, normalized by the total number of isolated dwarf galaxies in that stellar mass bin. Mass bins are selected as in Fig. 5. Mock multiples are selected based on either projected separations (*Projected*; red, dash–dotted) or by first requiring that the dwarfs have 3D separations less than 300 kpc (*Physical*; cyan, solid). The observed *SDSS* results are denoted in blue (dash–dotted). 1σ errors are indicated by the shaded regions. At the highest mass bin there is good agreement among all catalogues. At the lower mass bins the *Illustris Hydro Physical* has a lower rate of multiples than *SDSS*, whereas *Illustris Hydro Projected Projected* is a better match. Note that the higher N_c in the lowest mass bin in the *SDSS* catalogue may be a result of sensitivity bias towards galaxies that are bluer in colour, such as interacting dwarf pairs (there are only 130 dwarfs in that lowest mass bin).

Downloaded from https://academic.oup.com/mnras/article-abstract/480/3/3376/5063581 by California Institute of Technology user on 28 November 2018

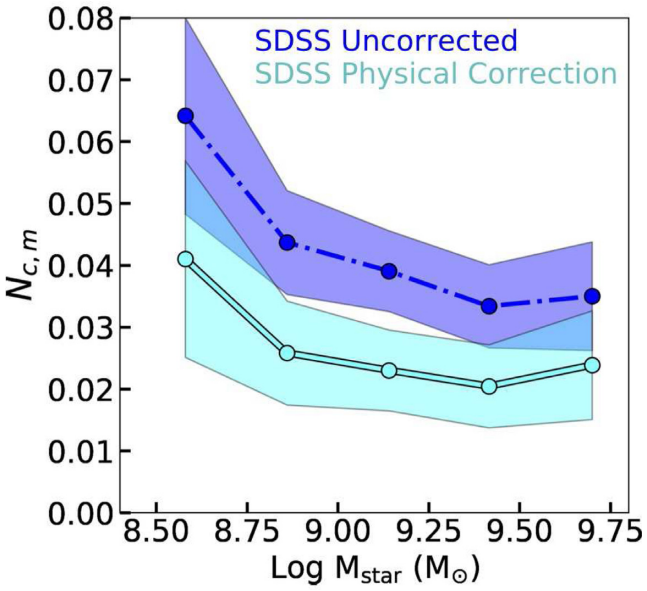

Figure 8. The original *SDSS* results for $N_{c,m}$ (blue, dash–dotted) are corrected for projection effects using the difference between $N_{c,m}$ for mock multiples selected using the *Illustris Hydro Projected* and *Illustris Hydro Physical* criteria from Fig. 7. The correction (cyan, solid line) is on average 30–40per cent per mass bin. We caution that the lowest mass bin for the *SDSS* results might overestimate the dwarf multiple fraction as *SDSS* sensitivity is biased to bluer galaxies. Interacting dwarfs are typically blue, making them easier to detect over their quiescent counterparts.

and thus bluer colours on average (see also Fig. 3). This suggests that dwarf multiples are easier to identify at the low-mass end than their non-interacting counterparts. Such observational bias would not be reflected in our mock dwarf selection criterion, where only limits on stellar mass, not colour, were implemented.

We use the fractional difference of $N_{c,m}$ between the *Illustris Hydro Physical* and *Illustris Hydro Projected* dwarf multiples in each mass bin to correct the *SDSS* results of Fig. 7 for projection effects. The result, plotted in Fig. 8, illustrates the predicted true $N_{c,m}$, if contaminants owing to projection effects were removed.

4.4 Frequency of pairs and groups

We define N_1 as the percentage of dwarfs with only one companion (a pair), N_2 as having only two companions (a triple) and N_3 as having three companions (a quad). In practice, we do not find higher order multiples in the catalogues. Note that with this definition, a true triple system, for example, would be counted three times, as there are three dwarfs that each have two companions. Results for all catalogues are summarized in Table 4.

Roughly 3.2 per cent of mock dwarfs in *Illustris Hydro Projected* are in a pair, meaning they have one companion within the stellar mass range afforded by our adopted sensitivity limits. This is within the 1σ errors of the *SDSS* value of 3.5 ± 0.3 per cent. This means that out of a sample of 10 000 isolated dwarfs, ∼150 unique pairs should exist in the mock sample and ∼175 in *SDSS*.

However, when mock dwarf multiples are required to have 3D separations <300 kpc (*Illustris Hydro Physical*) the fraction of mock pairs drops by ∼40 per cent. In other words, out of a sample of 10 000 isolated dwarfs, while there should be 175 projected pairs in *SDSS*, only ∼105 are cosmologically expected to have physical separations less than 300 kpc.

We find that very few dwarfs are found in a triple using any selection criteria in any catalogue (<0.2 per cent). Again, taking a sample of 10 000 isolated dwarfs, this fraction implies that at most ∼20 dwarfs have two companions, yielding 20/3 ∼7 unique projected triples.

In the *Illustris Hydro Physical* catalogue of multiples, not all sightlines through the simulation volume yield triples. Only ∼70 per cent of the 500 realizations of the *Illustris Hydro* volume yield any triples. Given the rarity of such configurations it is unsurprising that they are not identified in every realization of the catalogues. Results quoted in Table 4 are averaged over only sightlines where triples were identified.

Even fewer realizations of the mock catalogues (7 per cent in *Illustris Hydro Projected* and 2 per cent in *Illustris Hydro Physical*) yield dwarfs with three companions (quads). It is thus reasonable that none are identified in *SDSS*. Of those 2–7per cent of realizations, we find only 0.06 per cent of mock dwarfs with three companions. As such, for a sample of 10 000 isolated dwarfs, it is cosmologically expected that, at best, one may find one quad within our adopted mass constraints. Given that similar statistics are found using the Physical criteria, if a quad is identified under the same criteria as that adopted here, it is likely to be real.

We conclude that groups with more than three dwarf galaxy members (2×10^8 M$_\odot$ $< M_{star} < 5 \times 10^9$ M$_\odot$) with angular separations >55 arcsec, projected separations $r_p < 150$ kpc, and relative velocities < 150 km s^{-1} are very rare (<0.1 per cent) both cosmologically and observationally at low redshift ($z < 0.025$).

4.5 Predictions for next generation surveys: dwarf multiples with $M_{star} > 2 \times 10^8$ M$_\odot$

We create predictions for future photometric and spectroscopic surveys that are expected to be complete to stellar masses as low as $M_{star} = 2 \times 10^8$ M$_\odot$ within a (100 Mpc)^3 volume, such as LSST, DESI, etc. We do this by calibrating the *SDSS* multiples for completeness and projection effects using "complete" versions of the mock catalogues.

We remove the observational sensitivity limits (Fig. 3) in the mock dwarf selection criteria. Instead, we select all dwarfs with stellar masses $M_{star} > 2 \times 10^8$ M$_\odot$ in *Illustris Hydro* (where stellar mass is determined as in Section 2.2.1). Note that the *SDSS* catalogue is left unchanged. The new mock catalogue is called *Illustris Hydro Complete*.

Fig. 9 illustrates the distribution of stellar mass for the mock isolated dwarfs in the *Illustris Hydro Complete* catalogue as a function of redshift. Mock dwarfs are colour coded by their halo mass at $z = 0$. Plotted is one representative realization of the simulation volume.

Fig. 10 illustrates the corresponding fraction of dwarfs per stellar mass bin for *Illustris Hydro Complete* and the original *SDSS* results (where observational sensitivity limits are still enforced). The mock dwarf fraction increases towards lower masses, as expected.

We use the *Illustris Hydro Complete* catalogue to compute the average number of companions per mock dwarf galaxy (N_c) using the same *Projected* and *Physical* criteria listed in Section 4.1.1. Results are listed in Table 5, averaged over all 500 realizations of each catalogue. The fraction of mock dwarfs with companions has predictably increased in each mock catalogue. A discrepancy remains between the *Illustris Hydro Complete Projected* and *Illustris Hydro Complete Physical* catalogues, again indicating contamination from projection effects.

Downloaded from https://academic.oup.com/mnras/article-abstract/480/3/3376/5063581 by California Institute of Technology user on 28 November 2018

Table 4. Percentage of Dwarfs with a Given Number of Companions *Columns 3, 4, and 5)* N_1 indicates percentage of pairs, N_2 triples and N_3 quads. Note that very few sightlines through the *Illustris* volume host mock quads (only 2–7% of the 500 realizations of the simulation volume). The same is true for mock triples in *Illustris Hydro Physical* (50% of volume realizations host a triple). But mock triples are identified in 466 of 500 sightlines *Illustris Hydro Projected* and 475 of 500 realizations of the SDSS catalogue. Quoted is the fraction of mock dwarfs in such configurations averaged over all 500 catalogue realizations, regardless of whether a quad or triple was identified. *The Last Row)* indicates, for a sample of 10 000 isolated dwarfs, the number of expected *unique Projected* pairs, triples and quads, based on the largest percentage listed in the rows above (see text in Section 4).

Catalogue	Method	N_1	N_2	N_3
SDSS	Projected	3.5 ± 0.3	0.21 ± 0.08	none
Illustris Hydro	Projected	3.2 ± 0.5	0.10 ± 0.08	0.004 ± 0.003
Illustris Hydro	Physical	2.0 ± 0.4	0.08 ± 0.06	0.06 ± 0.03
10,000 Dwarfs	Projected, Max	∼160 Pairs	∼3 Triples	$\lesssim$1 Quad

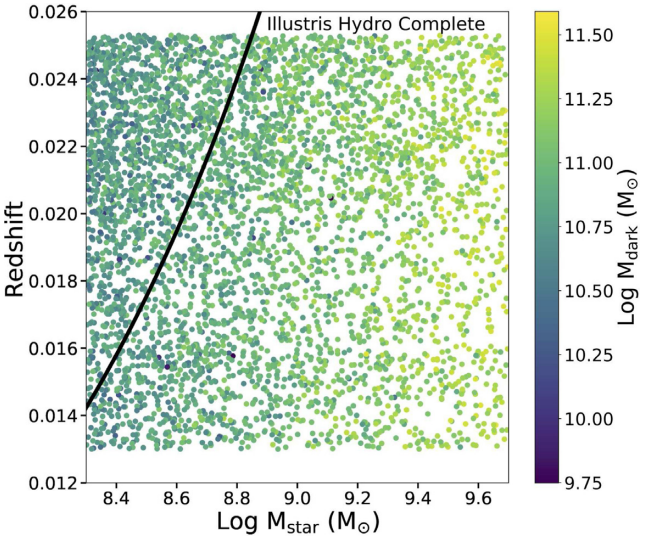

Figure 9. Distribution of stellar mass for mock isolated dwarfs in the *Illustris Hydro Complete* catalogue as a function of redshift for one representative realization of the simulation volume. This is the same plot as the right-hand panel of Fig. 3, but the observational sensitivity limits (black line) are no longer enforced for the mock catalogue. Instead, mock dwarfs are required to have a hard lower stellar mass limit of $M_{star} > 2 \times 10^8$ M$_\odot$.

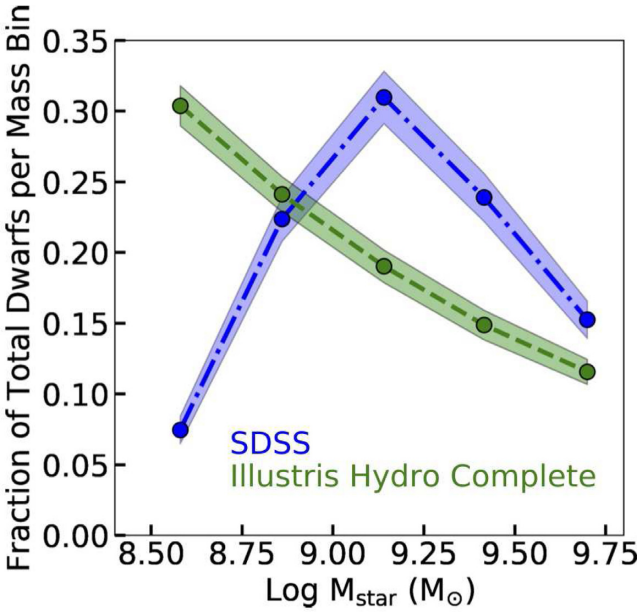

Figure 10. The fraction of isolated dwarf galaxies per stellar mass bin, relative to the total number of dwarf galaxies in each respective catalogue. This is similar to Fig. 5, but with observational sensitivity limits removed for the mock catalogues (corresponding to Fig. 9). The *SDSS* catalogue is unchanged relative to Fig. 5 (blue; dash–dotted). The mock galaxy results for *Illustris Hydro Complete* are plotted in green. 2σ errors are indicated by the shaded regions. Without sensitivity limits, the fraction of mock dwarfs grows sharply towards lower masses.

We calibrate the *SDSS* dwarf catalogue to account for survey incompleteness using the fractional difference between the *Illustris Hydro Projected* and *Illustris Hydro Complete Projected* results (denoted as *f*). The difference in N_c (Table 5/Table 3) for the mock *Projected* catalogue is $f \sim 1.4$. This increases predictions for a complete observational survey to $N_c \sim 0.06$ (last row of Table 5).

If we further include a correction for projection effects, we expect the number of multiples to decrease by ∼40 per cent (e.g. Fig. 8), yielding $N_c \sim 0.04$.

Fig. 11 plots the mean number of companions per mass bin, $N_{c,m}$, using both the *Illustris Hydro Complete Physical* and *Illustris Hydro Complete Projected* catalogues. This is similar to Fig. 7, but now using the complete mock catalogues. The *SDSS* results (blue) are unchanged, reflecting the original sensitivity limits of the survey. In both mock catalogues, $N_{c,m}$ increases for the most massive dwarf bins and decreases for low-mass bins. This is because the number of mock dwarfs in the lowest mass bins has increased substantially (Fig. 10). This result supports the hypothesis that the upturn in the *SDSS* results at low-mass bins is likely a result of survey incompleteness.

We now calibrate the *SDSS* results to predict $N_{c,m}$ for future observational surveys that will be complete to low masses. We compute the fractional change in $N_{c,m}$ between the *Illustris Hydro Projected* catalogues *without* the sensitivity limits (Fig. 11) and *with* them (Fig. 7) in each mass bin. In Fig. 12, we utilize this fractional change to correct the *SDSS* $N_{c,m}$ for completeness (green; dashed).

The *SDSS Completeness Correction* (green; dashed) results for $N_{c,m}$ are relatively flat across all mass bins at an average value of ∼0.06. This is the prediction for the mean number of companions per dwarf galaxy in future surveys that are complete to stellar masses of 2×10^8 M$_\odot$ over a ∼(100 Mpc)^3 volume.

5 DISCUSSION

In the following, we use the *SDSS* and mock dwarf-multiple catalogues to connect with existing studies of dwarf-–dwarf interactions in the literature. We first quantify the frequency of "Major Pairs" compared to studies of the "Major Merger" rate of dwarf galaxies (Section 5.1). We next quantify the observed and cosmologically expected frequency of analogues of the Magellanic Clouds in the

Downloaded from https://academic.oup.com/mnras/article-abstract/480/3/3376/5063581 by California Institute of Technology user on 28 November 2018

Table 5. Average N_c using Catalogues Complete to $M_{\rm star} > 2 \times 10^8$ M$_\odot$ Same as Table 3 except that a stellar mass floor of $M_{\rm star} > 2 \times 10^8$ M$_\odot$ has been applied to the mock catalogues. The *SDSS* result is unchanged and is listed for reference. *Column 4) f* indicates the fractional difference in N_c between each complete catalogue and their incomplete counterpart from Table 3. *The Last Row* is the expected N_c for projected multiples in *SDSS* if it were complete to $M_{\rm star} > 2 \times 10^8$ M$_\odot$.

Catalogue	Method	N_c	f
SDSS	Projected	0.039 ± 0.003	N/A
Illustris Hydro Complete	Projected	0.048 ± 0.005	1.4
Illustris Hydro Complete	Physical	0.032 ± 0.004	∼1.5
SDSS-Complete Correction	Projected	∼0.06	1.4

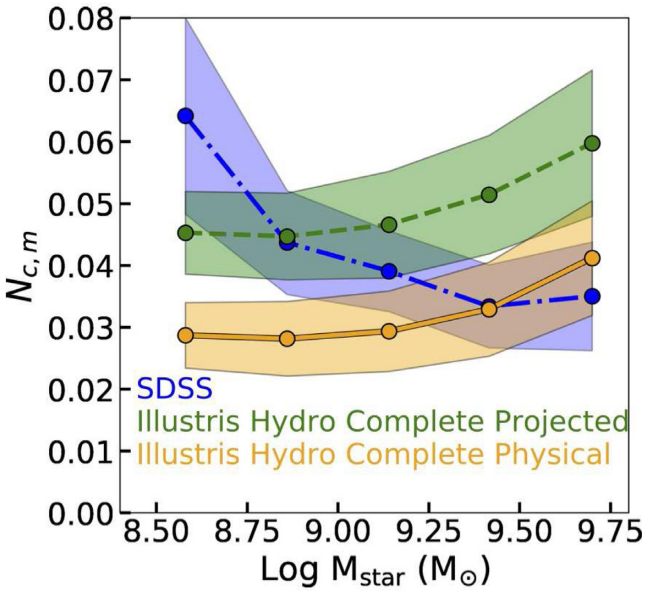

Figure 11. Same as Fig. 7 except that the sensitivity limits have been removed for the mock catalogues. Instead a stellar mass floor of $M_{\rm star} > 2 \times 10^8$ M$_\odot$ is applied to the mock catalogues (orange/solid and green/dashed lines). The *SDSS* catalogue result (blue; dashed–dotted) is unchanged. In both mock-complete catalogues, N_c decreases steadily towards lower mass bins, as expected given the increased sample size at low masses. Correspondingly, N_c increases at high masses relative to the incomplete catalogues in Fig. 7.

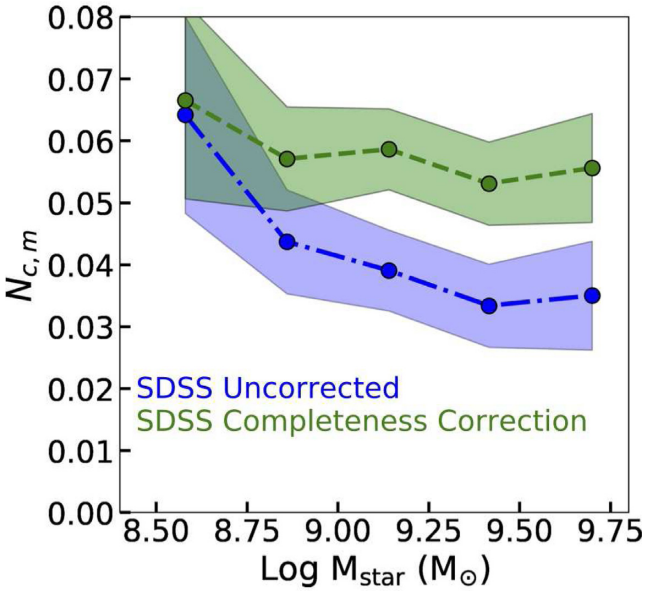

Figure 12. As in Fig. 7, we plot $N_{c,m}$, the average fractional number of dwarf companions per stellar mass bin. The original *SDSS* catalogue results are plotted in blue (dashed–dotted) and corrected for completeness (green; dashed). Corrections are made by multiplying the original *SDSS* results by the fractional change in $N_{c,m}$ computed for the *Illustris Hydro Projected* catalogues with or without the observational sensitivity limits (i.e. the ratio of the mock catalogues in Figs 7 and 11). The resulting *SDSS Completeness Correction* catalogue is relatively flat across all stellar mass bins at an average value of $N_{c,m} \sim 0.06$, in agreement with the average results in Table 5. Note that results for the lowest mass bin should be viewed cautiously as there may be a bias in the *SDSS* catalogue towards preferentially identifying multiples owing to their bluer colour. The cosmological samples suggest instead that the fraction should decrease at lower masses (see Fig. 11) for the adopted catalogue mass range.

field, comparing our results to the known frequency of such analogues near Milky Way type hosts (Section 5.2). Finally we place the recently discovered set of seven projected dwarf groups from the TiNy Titans (*TNT*) survey (Stierwalt et al. 2017) within the context of our study (Section 5.3).

5.1 "Major Pair" fraction, $M_{\rm S,\,star}/M_{\rm P,\,star} > 1/4$

Galaxy interactions are more destructive as the mass ratio of the interacting systems increases. We define destructive "Major Pairs" as dwarf galaxy pairs with stellar mass ratios of $M_{\rm S,\,star}/M_{\rm P,\,star} > 1/4$. S, star refers to stellar mass of the 2nd most massive member (Secondary) and P,star to that of the most massive member (Primary).

Fig. 13 illustrates the cumulative probability distribution of stellar mass ratios of dwarf pairs identified in the *SDSS* and *Illustris Hydro Physical* catalogues. Results for the *Illustris Hydro Projected* catalogue are similar; the stellar mass ratio distribution is unaffected by projection effects. We find that, within our adopted stellar mass and sensitivity limits, 70–85per cent of dwarf pairs identified in all catalogues are "Major Pairs".

The large fraction of high-mass ratio encounters is partly a result of our sensitivity and mass limits. Results for the *Illustris Hydro Physical Complete* catalogue is plotted in Fig. 13, where the sensitivity limits are dropped (as in Section 4.5). Now 60–70per cent of dwarf pairs are "Major Pairs". This fraction is certain to decrease as the mass limits of our surveys are lowered. As such, the stellar mass ratio distribution should not be confused/compared with a "complete" mass ratio distribution (e.g. figs 6 and 7 from Rodriguez-Gomez et al. (2015), bottom panels).

Fig. 14 plots $f_{\rm major}$, the number of all dwarf Primaries in a given stellar mass bin that have a Secondary dwarf galaxy companion

Downloaded from https://academic.oup.com/mnras/article-abstract/480/3/3376/5063581 by California Institute of Technology user on 28 November 2018

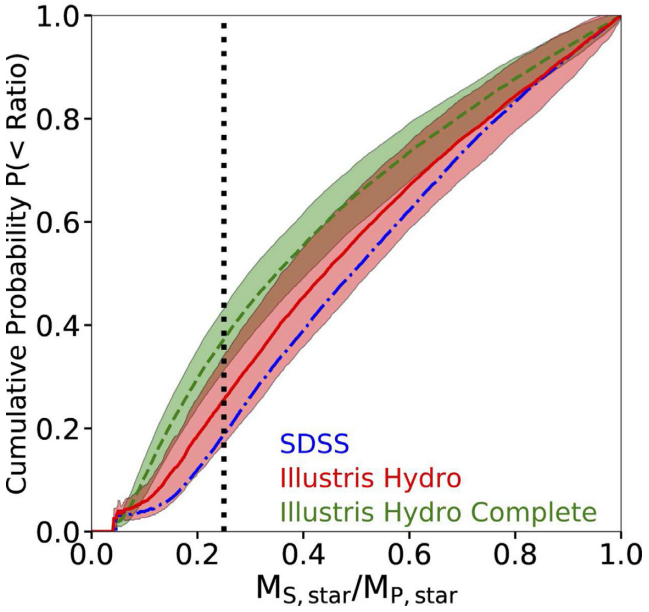

Figure 13. The cumulative probability distribution of the stellar mass ratio of Secondaries/Primaries ($M_{S,\,star}/M_{P,\,star}$) is plotted for multiples in the *SDSS* catalogue (blue; dash–dotted) and *Illustris Hydro Physical* catalogue (red; solid line). Results for *Illustris Hydro Projected* are similar. The shaded regions indicate 1σ deviation of the mean, computed over 500 realizations of each catalogue (SDSS errors are encompassed within the red shaded region). 70–85per cent of all pairs in the sensitivity limited catalogues are "Major Pairs", defined as having $M_{S,\,star}/M_{P,\,star} > 1/4$ (to the right of the limit denoted by the black dotted line). Results for *Illustris Hydro Physical Complete* (green; dashed line), indicate that for catalogues that are complete to $M_{star} = 2 \times 10^8$ $M_\odot$, "Major Pairs" are cosmologically expected to comprise 60–70per cent of the catalogue.

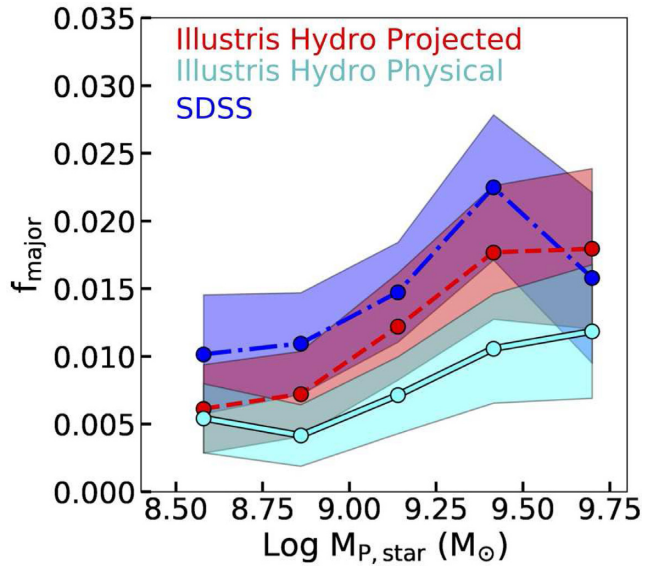

Figure 14. The Number of Primary dwarf galaxies that have a Secondary with a stellar mass ratio of $M_{S,\,star}/M_{P,\,star} > 1/4$ ("Major Pairs") per Primary stellar mass bin, normalized by the total number of isolated dwarf galaxies in that stellar mass bin (f_{major}). Mass bins are defined as in Fig. 7. Results for the *Illustris Hydro Projected* catalogue are in red (dashed line) and *Illustris Hydro Physical* in cyan (solid line). *SDSS* results are shown in blue (dash–dotted). Shaded regions indicate 1σ errors and lines the mean values. *Illustris Hydro Projected* results agree best with the *SDSS* catalogue. The "Major Pair" fraction at high mass (Log $M_{star} > 9.2$) is 1.2–2.5per cent; this is a robust result, as all catalogues are roughly complete at these masses.

with a stellar mass ratio of $M_{S,\,star}/M_{P,\,star} > 1/4$, normalized by the total number of dwarfs in the bin. Good agreement is found between the *SDSS* and *Illustris Hydro Projected* catalogues: the "Major Pair" fraction peaks at high-Primary masses at a value of $f_{major} \sim 0.02$ and steadily declines towards lower Primary masses, reaching a value of $f_{major} \sim 0.01$. The *Illustris Hydro Physical* catalogue shows the same qualitative behaviour, but with lower values.

In Fig. 15, we assess how much incompleteness has affected our results using the *Illustris Hydro Complete Projected* and *Physical* catalogues, where sensitivity limits are removed and only a stellar mass floor of 2×10^8 $M_\odot$ is enforced (see Section 4.5). Both complete mock catalogues show the same qualitative behaviour. The complete mock "Major Pair" fraction stays roughly flat between Primary stellar masses $\sim$log $(M_{star}) = 9.1$–$9.4 M_\odot$ at an average value of $f_{major} \sim 0.02$ for *Illustris Hydro Complete Projected* and $f_{major} \sim 0.012$ for *Illustris Hydro Complete Physical*. This result is robust, as all catalogues are roughly complete at those masses.

Note that the sharp drop off at lower stellar mass bins is a direct result of the lower stellar mass limit, and is not physical.

We utilize these results to calibrate the *SDSS* "Major Pair" fraction for completeness using the fractional change in the *Illustris Hydro Projected* "Major Pair" fraction with (Fig. 14) and without (Fig. 15) the *SDSS* sensitivity limits. The result is plotted in the right-hand panel of Fig. 15: the "Major Pair" fraction is cosmologically expected to continuously increase towards lower Primary stellar masses (within Log $M_{P,\,star} = 9.0 - 9.75$). At lower Primary masses, the fraction levels off at $f_{major} \sim 0.027$, but this levelling off likely due to the lower stellar mass limits. This behaviour is qualitatively similar to that found by Casteels et al. (2014), who defined "Major Mergers" based on *galaxy pair* separation and asymmetry in the GAMA survey (Driver et al. 2009, 2011). Note, however that their study accounts for dwarfs in all environments, whereas we focus only on isolated systems.

Sales et al. (2013) find that the *average* satellite abundance is largely independent of Primary mass for galaxies with $M_{star} < 10^{10}$ $M_\odot$). Here, we find that that the frequency of *isolated* "Major Pairs" appears to be a strong function of Primary stellar mass. But this apparent conflict is not surprising, given the rarity of "Major Pair" configurations.

Rodriguez-Gomez et al. (2015) derived the galaxy–galaxy "Major Merger" rate using merger histories computed with the SUBLINK code and the *Illustris Hydro* simulation. This is distinct from our method, as they count coalesced systems, whereas we identify dwarf pairs as distinct subhaloes.[3] Rodriguez-Gomez et al. (2015) find that the "Major Merger" rate steadily declines with decreasing Primary stellar mass, whereas we find the opposite behaviour for "Major Pairs" at $z \sim 0$. This suggests that the galaxy merger time-scale is both a function of redshift (Snyder et al. 2017) and galaxy mass, even at dwarf mass scales (see also Kitzbichler & White 2008; Conselice 2006). Note that we consider only isolated "Major Pairs", whereas Rodriguez-Gomez et al. (2015) measure the "global Major Merger" rate, regardless of environment. It is plausible that environmental

[3]Note that deriving a "Major Merger" rate using our pair fractions is difficult as the orbital time-scales of interacting dwarfs are unknown. From studies of the Magellanic Clouds (stellar mass ratio $M_{S,\,star}/M_{P,\,star} = 0.1$) the time of coalescence can be very long (> 6 Gyr, Pearson et al. 2018; Besla et al. 2016, see also,). We defer calculations of merger rates to a future study where we will study the kinematics of our dwarf multiples and orbital time-scales in detail.

Downloaded from https://academic.oup.com/mnras/article-abstract/480/3/3376/5063581 by California Institute of Technology user on 28 November 2018

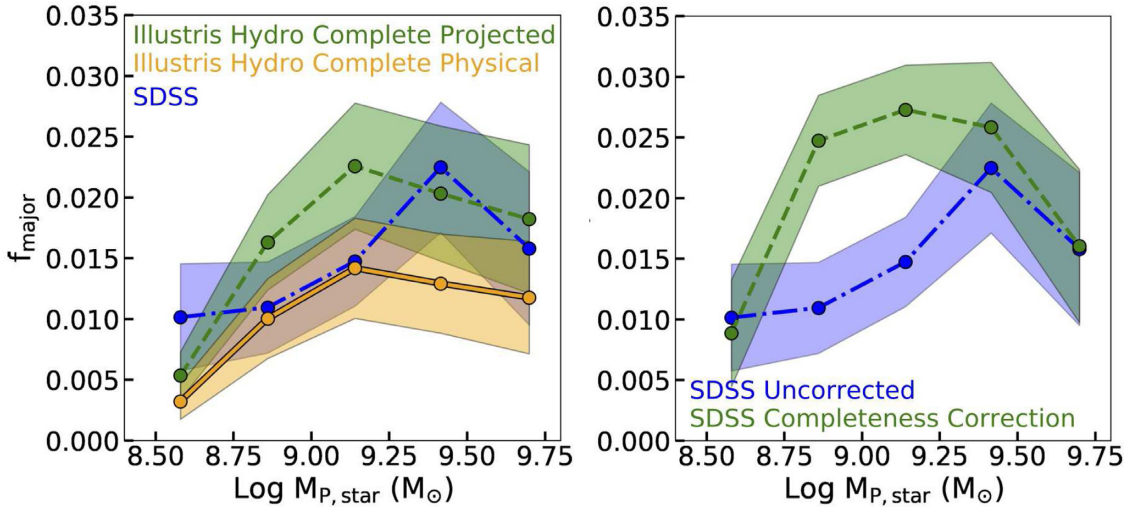

Figure 15. *Left:* Same as Fig. 14 except that the sensitivity limits have been removed for the mock catalogues. Instead, we require only a stellar mass floor of 2×10^8 $M_\odot$. *SDSS* results are unchanged (blue, dash–dotted). Note that the rapid drop in the lowest Primary mass bins results from a deficit of lower mass dwarfs in the catalogues. As expected, f_{major} does not change significantly for the most massive bin, which is roughly complete for all catalogues. In a complete catalogue, 1.8–2.5per cent of dwarfs with stellar masses in excess of 10^9 $M_\odot$ are cosmologically expected to be found in a projected "Major Pair". Accounting for pairs within a 300 kpc separation (*Illustris Hydro Complete Physical*) reduces these values by a factor of ∼1.7. *Right:* We correct the *SDSS* results for completeness (green, dashed line) using the fractional difference between the *Illustris Hydro Complete Projected* (left-hand panel) and *Illustris Hydro Projected* (Fig. 14) results per mass bin. The blue, dash-dotted line is the original *SDSS* results. Surveys like LSST are predicted to find a dwarf "Major Pair" fraction that increases with decreasing Primary stellar mass. The levelling off at $\sim 10^9$ $M_\odot$ likely owes to the lower stellar mass limit of the catalogues.

effects (e.g. the tidal field of the host) could impact the merger rate of dwarf pairs after capture by a more massive host.

Regardless, our result indicates that long term, repetitive dwarf–dwarf interactions may play an important role in the SFHs, the origin of starbursts and gas removal processes in isolated dwarf galaxies. Because dwarf galaxies in the field have significant gas fractions ($f_{gas} > 50$ per cent; Geha et al. 2012; Bradford et al. 2015), tidal interactions between dwarfs are more likely to remove gas than stars. The creation of extended, long-lived gas tidal structures around dwarf pairs will affect the nature of their circumgalactic medium and impact their baryon cycles, both in isolation and after accretion into a more massive environment (Pearson et al. 2018).

5.2 The frequency of isolated LMC & SMC analogues

The closest example of dwarf–dwarf galactic pre-processing at work is the Magellanic System. The interacting dwarf pair, the LMC and SMC, are enveloped by a massive (2×10^9 $M_\odot$; Fox et al. 2014) complex of gas called the Magellanic Stream, Bridge, and Leading Arm (Mathewson, Cleary & Murray 1974; Putman et al. 2003; Nidever et al. 2010). This extended gaseous complex is primarily created by the tidal interaction between the two dwarfs (Besla et al. 2010; Diaz & Bekki 2011; Besla et al. 2012; Besla et al. 2013; Guglielmo, Lewis & Bland-Hawthorn 2014; Pardy, D'Onghia & Fox 2018). Furthermore, orbital solutions indicate that the Clouds are recent interlopers to our Galaxy (Besla et al. 2007; Kallivayalil et al. 2013). This implies that the Magellanic Clouds must have been a relatively isolated, interacting galaxy pair prior to their capture by the Milky Way. This study is designed to determine whether such isolated dwarf pair configurations are expected cosmologically.

The frequency of analogues of the Magellanic Clouds about massive hosts has been quantified in both cosmological simulations and *SDSS*, finding good agreement. Roughly, 40 per cent of Milky Way analogues in both cosmological simulations and *SDSS* host an LMC-type galaxy (Boylan-Kolchin et al. 2011; Busha et al. 2011; Tollerud et al. 2011; Robotham et al. 2012; Patel, Besla & Sohn 2017). On the other hand, it is rare (∼2–5per cent) to find both an LMC and SMC analogue in proximity to a massive host (Boylan-Kolchin et al. 2011; Busha et al. 2011; Liu et al. 2011; Robotham et al. 2012; Gonzalez et al. 2013). The observational statistics become minuscule if one further requires a Milky Way-LMC-SMC analogue with clear signs of interaction between the two satellites or that the LMC/SMC analogues also be in close proximity to each other (James & Ivory 2011; Paudel & Sengupta 2017). However, the cosmologically expected frequency of LMC-SMC analogues (mass, separation, relative velocity) in the *field* is unknown.

From Fig. 13, we find that Primaries with companions of stellar mass ratios of 1:5 represent ∼20 per cent of each catalogue of dwarf multiples. We refine this analysis to identify LMC-SMC analogues with similar separations, stellar masses, and mass ratio as the real system. LMC analogues are defined as dwarfs with stellar masses of 10^9 $M_\odot$ $< M_{star} <$ 5×10^9 $M_\odot$. On average we find $\sim 1700 \pm 200$ dwarfs satisfying these criteria in *Illustris Hydro*. The standard deviation results from a combination of scatter in the abundance matching relations and variations in the number of dwarfs in different realizations of the simulation volume.

We define SMC analogues as those dwarfs with stellar mass ratios of 1:15 < LMC:SMC < 1:5 and projected separations of r_p < 100 kpc to an LMC analogue. Separation limits are motivated by Besla et al. (2012), who find a best-fitting orbit for the LMC/SMC with apocentres reaching such distances. Examples of the properties for LMC/SMC analogues in one realization of the *SDSS* and mock catalogues are plotted in Figs 1 and 6 where LMC/SMC analogues are marked by symbols with orange outlines.

For all samples, LMC analogues that host SMC analogues have, on average, present day dark matter subhalo masses a factor of 1.2–1.3times more massive than those that do not, in agreement with the recent study by Shao et al. (2018). This result supports high-mass

Downloaded from https://academic.oup.com/mnras/article-abstract/480/3/3376/5063581 by California Institute of Technology user on 28 November 2018

models for the total dark matter mass of the LMC when it first entered the Milky Way (Besla et al. 2012; Peñarrubia et al. 2016, Garavito-Camargo, Besla in preparation).

We further find that ∼0.2–0.3 per cent of LMC mass galaxies in the field host an SMC-like companion in both *SDSS* and *Illustris Hydro Projected* (averaged over 500 realizations of the catalogues). This result is confirmed in *Illustris Hydro Physical*, indicating that pairs selected with $r_p < 100$ kpc are robust to projection effects. Removing the observational sensitivity limits doubles the frequency of LMC/SMC analogues, but overall we find them to be very rare in the field (cosmologically and observationally). Of order 1 per cent of LMC analogues are expected to be found with an SMC-mass companion in a catalogue that is complete to SMC masses of $2 \times 10^8 M_\odot$.

Robotham et al. (2012) utilized the GAMA Survey to explore the frequency of LMC/SMC analogues as a function of environment. They found that ∼4.8 per cent of galaxies with $-19 < M_r < -17$ have a companion in this magnitude range within a projected separation of <100 kpc and velocity separation of $<100\,\mathrm{km\,s^{-1}}$ (46 out of 1929 galaxies). This is higher than what we find here, but their results consider a wider range of environments. These authors find a higher probability of finding LMC/SMC analogues in proximity of a Local Group analogue (within 1 Mpc). Indeed, half (27) of such pairs are within 1 Mpc of an L∗ galaxy and would fail our isolation criteria, where all dwarfs are at least 1.5 Mpc away from an L∗ type system. This reconciles our statistics with the GAMA study (<1 per cent of GAMA LMC/SMC analogues would pass our isolation criteria).

While we find that LMC/SMC configurations are rare today, it is possible that they have been more frequent at earlier times. The good agreement between the mock catalogues and *SDSS* indicate that cosmological simulations are reasonable tools to explore the kinematics and frequency of such configurations across cosmic time, an analysis that we defer to a later study.

5.3 The TNT dwarf groups in a cosmological context

The TiNy Titans (*TNT*) survey of dwarf galaxy pairs identified in *SDSS* at low redshift ($0.005 < z < 0.07$) showed that the SFRs of dwarf pairs increase with decreasing pair separation. This suggests that coalescence is not required to induce a burst of star formation. Moreover, the secondary galaxy was typically the pair member undergoing the starburst. Together, these results strongly suggest that the average dwarf galaxy multiple fractions (N_c) that we have determined in previous sections, are important to understanding the drivers of starbursts in dwarf galaxies.

Lee et al. (2009) find that 6 per cent of dwarfs within an 11 Mpc volume of the Milky Way are currently starbursting. In Section 4.5, we found that a comparable fraction (∼4 per cent) of isolated dwarfs in *SDSS* should have a dwarf galaxy companion with angular separations >55 arcsec, projected separations $r_p <$ 150 kpc, physical separations <300 kpc, and a relative velocity difference of $<150\,\mathrm{km\,s^{-1}}$.

Recently, Stierwalt et al. (2017) (hereafter S17) identified seven isolated groups of dwarfs with three members or more at low redshift, including a group with five members. All dwarf groups are identified to have projected separations less than 80 kpc and most have separations greater than 15 kpc. Furthermore, most dwarf members have velocities relative to the Primary that are less $200\,\mathrm{km\,s^{-1}}$. These properties are comparable to our selection criteria for the *SDSS* and *Illustris Hydro Projected* catalogues of dwarf multiples.

Note that loose associations of dwarfs have also been identified in the Local Volume (Tully et al. 2006), however they have much larger projected sizes (> 500 kpc) than we consider in this study.

In Section 4.4, we found it highly improbable to find groups of four members or more at low redshift. At first glance, these results seem at odds with S17. However, the dwarf stellar mass range explored in S17 extends to lower masses than we consider in this study. This coupled with our restrictive velocity cut of $<150\,\mathrm{km\,s^{-1}}$ reduces four of the dwarf groups in S17 to dwarf pairs and makes three companionless. As such, the findings from S17 are consistent with our study, where we find that dwarfs within our mass range are more likely to be in pairs, rather than larger multiples.

Unfortunately, because of the mass limits adopted in our study (motivated by the observational sensitivity limits of the *SDSS* survey and mass resolution limits of the simulations), we cannot state with certainty that the S17 groups containing dwarfs with masses below $\log(M_{\rm star}) = 8.3$ are consistent with cosmological expectations. Our results do suggest that high-speed members ($\Delta V > 150\,\mathrm{km\,s^{-1}}$) of quads or quints in the dwarf mass range explored in this study are likely projected contaminants. However, if quads are identified to satisfy the position and velocity ($\Delta V < 150\,\mathrm{km\,s^{-1}}$) constraints of this study, the agreement between the frequency of quad identification in *Illustris Hydro Projected* and *Illustris Hydro Physical* (see Section 4) do suggest that they are not chance alignments.

6 CONCLUSIONS

The frequency of companions to isolated dwarf galaxies ($M_{\rm star} = 2 \times 10^8$–$5 \times 10^9$ $M_\odot$) at low redshift ($0.013 < z < 0.0252$) is quantified in the *SDSS* Legacy spectroscopic catalogue (M14) and compared against cosmological expectations using mock catalogues constructed using the *Illustris-1* hydrodynamic cosmological simulation (*Illustris Hydro*). We have chosen stellar mass and redshift ranges where the cosmological and observed catalogues can be reasonably compared, accounting for both the resolution of the simulation and the sensitivity limits of *SDSS*.

We define dwarf galaxies to be isolated if no Massive Galaxy ($M_{\rm star} > 5 \times 10^9$ $M_\odot$) can be identified with both a relative velocity of $\Delta V_{\rm LOS} < 1000\,\mathrm{km\,s^{-1}}$ and a Tidal Index $\Theta > -14.9$ (Karachentsev et al. 2013).

Overall we find good agreement between *SDSS* and cosmological expectations for the fraction of dwarf multiples (pairs/groups) in isolated environments. Our main results are summarized in the following.

(i) **There are more dwarfs in the field in the cosmological simulations relative to *SDSS*.** We confirm results from Klypin et al. (2015) that the abundance of mock dwarf galaxies in the field is higher than observed. Using *Illustris Hydro*, we find densities ∼2.0 times higher than in *SDSS* (Table 2). This overabundance of field dwarfs (where environmental effects are negligible) may indicate that many low-surface brightness dwarfs are currently missing from the *SDSS* spectroscopic catalogue (Greco et al. 2017; Danieli et al. 2018), or may be reconciled with improved subgrid physics models (Wetzel et al. 2016) and the inclusion of reionization. Regardless, the solution must be consistent across the dwarf stellar mass range, as a similar fraction of dwarfs are missing in each mass bin, which may be challenging.

(ii) **The fraction of isolated dwarfs as a function of stellar mass in *SDSS* agrees with cosmological expectations,** (see Fig. 5). We thus focus our study on the fraction of dwarfs found in a multiple (pairs, triples, quads, etc.).

Downloaded from https://academic.oup.com/mnras/article-abstract/480/3/3376/5063581 by California Institute of Technology user on 28 November 2018

(iii) **The mean number of companions per isolated dwarf is $N_c \sim 0.04$.** We identify dwarf companions based on the following *Projected* criteria: 1) an angular separations of >55 arcsec and a projected separation of $r_p < 150$ kpc; and 2) a relative line-of-sight velocity of $\Delta V_{LOS} < 150\,km\,s^{-1}$. Following the methodology of Patton et al. (2000) and applying these *Projected* criteria, we find the mean number of low-mass companions per dwarf to be $N_c = 0.039 \pm 0.003$ in *SDSS*, which agrees within 1σ of the cosmological catalogue ($N_c = 0.034 \pm 0.005$ for *Illustris Hydro Projected*). These fractions are certain to be higher if lower stellar mass companions were considered in this study.

(iv) **~40 per cent of isolated dwarf multiples are false associations owing to projection effects.** To assess the degree of contamination from projected pairs with large 3D separations, we add a requirement that all companions have a 3D separation of r_{3D} <300 kpc (*Illustris Hydro Physical*). This reduces N_c by 40 per cent, indicating a significant contamination fraction exists when selecting dwarf pairs based on projected properties. We calibrate the *SDSS* findings for contamination from such projection effects, finding a true average fractional number of physical companions per dwarf to be $N_c = 0.027$.

(v) **The majority of isolated dwarf multiples in our mass range are Pairs. Triples are rare and higher order multiples are cosmologically improbable within our adopted redshift, mass, separation, and relative velocity limits.** Less than 0.2 per cent of mock or observed isolated dwarfs are found in a triple. Most mock triples in our mass range contain projected contaminants; most high-order multiples are no longer identified when dwarf companions are required to have 3D separations < 300 kpc *Illustris Hydro Physical*.

(vi) **The recently discovered *TNT* groups (S17) are reconcilable with cosmological expectations.** Our results do not conflict with the recent discovery of seven high-order dwarf multiples by the *TNT* group (S17), as most members of those groups would not satisfy our selection criteria, either owing to their low-stellar mass or high-relative speed, which reduce the groups to pairs or single dwarfs according to our selection criteria.

(vii) **We predict the average number of companions per isolated dwarf to be $N_c \sim 0.06$ in future surveys that are complete to $M_{star} = 2 \times 10^8\,M_\odot$.** We remove sensitivity limits to construct mock galaxy catalogues, applying instead a stellar mass floor of $M_{star} = 2 \times 10^8\,M_\odot$. This increases the fraction of multiples by a factor of $f \sim 1.4$ in *Illustris Projected Hydro* ($N_c = 0.048 \pm 0.005$). We utilize this result to calibrate the observed fraction of dwarf multiples in *SDSS* for future surveys, finding an expected average fraction of *Projected* companions per dwarf of $N_c = 0.06$. This value is expected to be roughly constant across the entire dwarf mass range explored in this study. Testing these predictions will require a spectroscopic complement to deep photometric imaging surveys (e.g. the combination of both LSST and DESI).

(viii) **<1 per cent of isolated LMC analogues have an SMC-like companion.** For surveys complete to $M_{star} = 2 \times 10^8\,M_\odot$ (i.e. the stellar mass of the SMC) out to 100 Mpc, the cosmological catalogues indicate that 1 per cent of LMC mass analogues are expected to have an SMC-like companion (stellar mass ratio of 1:5–1:15 and $r_p < 100$ kpc). This is in agreement with the *SDSS* catalogues and results from the GAMA survey (Robotham et al. 2012). We conclude that analogues of the LMC and SMC pair are rare in the field at low z.

(ix) **The fraction of isolated "Major Pairs" increases with decreasing stellar mass in the dwarf regime.** We find good agreement between the fraction of "Major Pairs", dwarf pairs with stellar mass ratios >1: 4, in *SDSS* and *Illustris Hydro Projected* (Fig. 14). Correcting the *SDSS* catalogue for completeness, the "Major Pair" fraction increases with decreasing stellar mass, from $f_{major} \sim 0.015$ at ~LMC masses to f_{major} ~0.027 at lower masses. This is the opposite behaviour of the cosmological "Major Merger" rate, defined by the coalescence of two galaxies identified by the extracted merger trees for each decendent halo (Rodriguez-Gomez et al. 2015). This suggests that the merger time-scales for dwarfs are not only redshift-dependent (Snyder et al. 2017) but also mass dependent.

The good agreement between observations and cosmological expectations for the fraction of dwarf multiples at $z = 0$ indicates that we can reasonably utilize the kinematic properties of cosmological dwarfs multiples to understand their dynamical state and merger time-scales across cosmic time.

ACKNOWLEDGEMENTS

We thank Marla Geha, Greg Snyder, and Nicolas Garavito-Camargo for useful conversations that have facilitated this work. We also thank the *Illustris* collaboration for making their subhalo catalogues and merger trees publicly available.

GB acknowledges that this material is based on work supported by the National Science Foundation under grant AST 1714979. NK is supported by NSF CAREER award 1455260. DRP acknowledges the support of the Natural Sciences and Engineering Research Council of Canada (NSERC).

The analysis in this study was carried out using the El Gato cluster at the University of Arizona, which is funded by the National Science Foundation through Grant No. 1228509.

This work has also used catalogues from the NASA Sloan Atlas and the SDSS. Funding for the NASA Sloan Atlas has been provided by the NASA Astrophysics Data Analysis Program (08-ADP08-0072) and the NSF (AST- 1211644).

Funding for SDSS-III has been provided by the Alfred P. Sloan Foundation, the Participating Institutions, the National Science Foundation, and the U.S. Department of Energy Office of Science. The SDSS-III web site is http://www.sdss3.org/.

SDSS-III is managed by the Astrophysical Research Consortium for the Participating Institutions of the SDSS-III Collaboration including the University of Arizona, the Brazilian Participation Group, Brookhaven National Laboratory, Carnegie Mellon University, University of Florida, the French Participation Group, the German Participation Group, Harvard University, the Instituto de Astrofisica de Canarias, the Michigan State/Notre Dame/JINA Participation Group, Johns Hopkins University, Lawrence Berkeley National Laboratory, Max Planck Institute for Astrophysics, Max Planck Institute for Extraterrestrial Physics, New Mexico State University, New York University, Ohio State University, Pennsylvania State University, University of Portsmouth, Princeton University, the Spanish Participation Group, University of Tokyo, University of Utah, Vanderbilt University, University of Virginia, University of Washington, and Yale University.

This research also utilized: IPython (Perez & Granger 2007), numpy (van der Walt, Colbert & Varoquaux 2011), and matplotlib (Hunter 2007).

REFERENCES

Abazajian K. N. et al., 2009, ApJS, 192, 543
Behroozi P. S. et al., 2015, MNRAS, 450, 1546
Bell E. F., Phleps S., Somerville R. S., Wolf C., Borch A., Meisenheimer K., 2006, ApJ, 652, 270

Downloaded from https://academic.oup.com/mnras/article-abstract/480/3/3376/5063581 by California Institute of Technology user on 28 November 2018

Berrier J. C., Bullock J. S., Barton E. J., Guenther H. D., Zentner A. R., Wechsler R. H., 2006, ApJ, 652, 56
Besla G., Kallivayalil N., Hernquist L., Robertson B., Cox T. J., van der Marel R. P., Alcock C., 2007, ApJ, 668, 949
Besla G., Kallivayalil N., Hernquist L., van der Marel R. P., Cox T. J., Keres D., 2010, ApJ, 721, L97
Besla G., Kallivayalil N., Hernquist L., van der Marel R. P., Cox T. J., Keres D., 2012, MNRAS, 421, 2109
Besla G., Hernquist L., Loeb A., 2013, MNRAS, 428, 2342
Besla G., Martínez-Delgado D., van der Marel R. P., Beletsky Y., Seibert M., Schlafly E. F., Grebel E. K., Neyer F., 2016, ApJ, 825, 20
Binggeli B., Sandage A., Tammann G. A., 1988, ARA&A, 26, 509
Blanton M. R., Lupton R. H., Schlegel D. J., Strauss M. A., Brinkmann J., Fukugita M., Loveday J., 2005, ApJ, 631, 208
Blumenthal G. R., Faber S. M., Primack J. R., Rees M. J., 1984, Nature, 311, 517
Boylan-Kolchn M., Besla G., Hernquist L., 2011, MNRAS, 414, 1560
Bradford J. D., Geha M. C., Blanton M. R., 2015, ApJ, 809, 146
Bundy K., Fukugita M., Ellis R. S., Kodama T., Conselice C. J., 2004, ApJ, 601, L123
Busha M. T., Marshall P. J., Wechsler R. H., Klypin A., Primack J., 2011, ApJ, 743, 40
Carlberg R. G. et al., 2000, ApJ, 532, L1
Casteels K. R. V. et al., 2014, MNRAS, 445, 1157
Chua K. T. E., Pillepich A., Rodriguez-Gomez V., Vogelsberger M., Bird S., Hernquist L., 2017, MNRAS, 472, 4343
Conselice C. J., 2006, ApJ, 638, 686
Conselice C. J., Bershady M. A., Dickinson M., Papovich C., 2003, AJ, 126, 1183
Cui W., Borgani S., Dolag K., Murante G., Tornatore L., 2012, MNRAS, 423, 2279
Danieli S., van Dokkum P., Conroy C., 2018, ApJ, 856, 69
Deason A. J., Wetzel A. R., Garrison-Kimmel S., Belokurov V., 2015, MNRAS, 453, 3568
Di Cintio A., Brook C. B., Dutton A. A., Macciò A. V., Stinson G. S., Knebe A., 2014, MNRAS, 441, 2986
Diaz J., Bekki K., 2011, MNRAS, 413, 2015
Dolag K., Borgani S., Murante G., Springel V., 2009, MNRAS, 399, 497
Dooley G. A., Peter A. H. G., Carlin J. L., Frebel A., Bechtol K., Willman B., 2017, MNRAS, 472, 1060
Driver S. P. et al., 2009, Astron. & Geophys., 50, 5.12
Driver S. P. et al., 2011, MNRAS, 413, 971
Fattahi A., Navarro J. F., Starkenburg E., Barber C. R., McConnachi A. W., 2010, MNRAS, 431, L73
Fox A. J., et al., 2014, ApJ, 787, 147
Geha M., Blanton M. R., Masjedi M., West A. A., 2006, ApJ, 653, 240
Geha M., Blanton M. R., Yan R., Tinker J. L., 2012, ApJ, 757, 85
Genel S. et al., 2014, MNRAS, 445, 175
González R. E., Padilla N. D., 2016, ApJ, 829, 58
Gonzalez R. E., Kravtsov A. V., Gnedin N. Y., 2013, ApJ, 770, 96
Grcevich J., Putman M. E., 2009, ApJ, 696, 385
Greco J. P. et al., 2018, ApJ, 857, 104
Guglielmo M., Lewis G. F., Bland-Hawthorn J., 2014, MNRAS, 444, 1759
Guo Q., White S. D. M., 2008, MNRAS, 384, 2
Harris J., Zaritsky D., 2006, AJ, 131, 2514
Hinshaw G. et al., 2013, ApJS, 208, 19
Hopkins P. F. et al., 2010, ApJ, 724, 915
Hunter J. D., 2007, Comput. Sci. Eng., 9, 90
James P. A., Ivory C. F., 2011, MNRAS, 411, 495
Kallivayalil N., van der Marel R. P., Besla G., Anderson J., Alcock C., 2013, ApJ, 764, 161
Karachentsev I. D., Karachentseva V E., Huchtmeier W. K., Makarov D. I., 2004, AJ, 127, 2031
Karachentsev I. D., Makarov D. I., Kaisina E. I., 2013, AJ, 145, 101
Kitzbichler M. G., White S. D. M., 2008, MNRAS, 391, 1489
Klypin A., Karachentsev I., Makarov D., Nasonova O., 2015, MNRAS, 454, 1798
Kravtsov A. V., 2010, Adv. Astron., 2010, 1
Lacey C., Cole S., 1993, MNRAS, 262, 627
Lee J. C., Kennicutt R. C., Funes S. J. J. G., Sakai S., Akiyama S., 2009, ApJ, 692, 1305
Lelli F., Fraternali F., Verheijen M., 2014, A&A, 563, A27
Lin L. et al., 2008, ApJ, 681, 232
Liu L., Gerke B. F., Wechsler R. H., Behroozi P. S., Busha M. T., 2011, ApJ, 733, 62
Lotz J. M., Johnsson P., Cox T. J., Croton D., Primack J. R., Somerville R. S., Stewart K., 2011, ApJ, 742, 103
Man A. W. S., Zirm A. W., Toft S., 2016, ApJ, 830, 89
Mantha K. B. et al., 2018, MNRAS, 475, 1549
Marasco A., Crain R. A., Schaye J., Bahe Y. M., van der Hulst T., Theuns T., Bower R. G., 2016, MNRAS, 461, 2630
Mathewson D. S., Cleary M. N., Murray J. D., 1974, ApJ, 190, 291
McConnachie A. W., Ellison S. L., Patton D. R., 2008, MNRAS, 387, 1281
Mendel J. T., Simard L., Palmer M., Ellison S. L., Patton D. R., 2014, ApJS, 210, 3 (M14)
Moster B. P., Naab T., White S. D. M., 2013, MNRAS, 428, 3121
Mundy C. J., Conselice C. J., Duncan K. J., Almaini O., Häußler B., Hartley W. G., 2017, MNRAS, 470, 3507
Nelson D. et al., 2015, Astron. Comput., 13, 12
Nidever D. L., Majewski S. R., Burton W. B., Nigra L., 2010, ApJ, 723, 1618
Noeske K. G., Iglesias-Páramo J., Vílchez J. M., Papaderos P., Fricke K. J., 2001, A&A, 371, 806
Odewahn S. C., 1994, AJ, 107, 1320
Pardy S. A., D'Onghia E., Fox A. J., 2018, *ApJ*, 857, 101
Patel E., Besla G., Sohn S. T., 2017, MNRAS, 464, 3825
Patton D. R., Atfield J. E., 2008, ApJ, 685, 235
Patton D. R., Carlberg R. G., Marzke R. O., Pritchet C. J., da Costa L. N., Pellegrini P. S., 2000, ApJ, 536, 153
Patton D. R. et al., 2002, ApJ, 565, 208
Patton D. R., Torrey P., Ellison S. L., Mendel J. T., Scudder J. M., 2013, MNRAS, 433, L59
Patton D. R., Qamar F. D., Ellison S. L., Bluck A. F. L., Simard L., Mendel J. T., Moreno J., Torrey P., 2016, MNRAS, 461, 2589
Paudel S., Sengupta C., 2017, ApJ, 849, L28
Pearson S. et al., 2016, MNRAS, 459, 1827
Pearson S. et al., 2018, preprint (arXiv:1807.03791)
Peñarrubia J., Gómez F. A., Besla G., Erkal D., Ma Y.-Z., 2016, MNRAS, 456, L54
Peng Y.-J. et al., 2010, ApJ, 721, 193
Perez F., Granger B. E., 2007, Comput. Sci. Eng., 9, 21
Privon G. C. et al., 2017, MNRAS, 468, 885
Putman M. E., Staveley-Smith L., Freeman K. C., Gibson B. K., Barnes D. G., 2003, ApJ, 586, 170
Robotham A. S. G. et al., 2012, MNRAS, 424, 1448
Rodriguez-Gomez V. et al., 2015, MNRAS, 449, 49
Sales L. V., Wang W., White S. D. M., Navarro J. F., 2013, MNRAS, 428, 573
Sánchez-Janssen R. et al., 2013, A&A, 554, A20
Sawala T., Frenk C. S., Crain R. A., Jenkins A., Schaye J., Theuns T., Zavala J., 2013, MNRAS, 431, 1366
Schaye J. et al., 2015, MNRAS, 446, 521
Shao S., Cautun M., Deason A. J., Frenk C. S., Thenus T., 2018, *MNRAS*, 479, 284
Simard L., Mendel J. T., Patton D. R., Ellison S. L., McConnachie A. W., 2011, ApJS, 196, 11
Snyder G. F., Lotz J. M., Rodriguez-Gomez V., Guimarães R. da S., Torrey P., Hernquist L., 2017, MNRAS, 468, 207
Spekkens K., Urbancic N., Mason B. S., Willman B., Aguirre J. E., 2014, ApJ, 795, L5
Springel V., White S. D. M., Tormen G., Kauffmann G., 2001, MNRAS, 328, 726
Springel V. et al., 2017, MNRAS, 475, 676
Stanimirović S., Staveley-Smith L., Jones P. A., 2004, ApJ, 604, 176
Stierwalt S., Besla G., Patton D., Johnson K., Kallivayalil N., Putman M., Privon G., Ross G., 2015, ApJ, 805, 2

Downloaded from https://academic.oup.com/mnras/article-abstract/480/3/3376/5063581 by California Institute of Technology user on 28 November 2018

Stierwalt S., Liss S. E., Johnson K. E., Patton D. R., Privon G. C., Besla G., Kallivayalil N., Putman M., 2017, Nature Astron., 1, 0025 (S17)
Tollerud E. J., Boylan-Kolchin M., Barton E. J., Bullock J. S., Trinh C. Q., 2011, ApJ, 738, 102
Tully R. B. et al., 2006, AJ, 132, 729
van den Bergh S., 2006, AJ, 132, 1571
van der Marel R. P., Kallivayalil N., 2014, ApJ, 781, 121
van der Marel R. P., Alves D. R., Hardy E., Suntzeff N. B., 2002, AJ, 124, 2639
van der Marel R. P., Kallivayalil N., Besla G., 2009, in van Loon J. T., Oliveira J. M., eds, Proc. IAU Symp. 256, The Magellanic System: Stars, Gas and Galaxies. Cambridge Univ. Press, Cambridge, p. 81
van der Walt S., Colbert S. C., Varoquaux G., 2011, Comput. Sci. Eng., 13, 22
Ventou E. et al., 2017, A&A, 608, A9
Vogelsberger M. et al., 2014, Nature, 509, 177
Weisz D. R. et al., 2011, ApJ, 739, 5
Wellons S., Torrey P., 2017, MNRAS, 467, 3887
Wetzel A. R., Deason A. J., Garrison-Kimmel S., 2015, ApJ, 807, 49
Wetzel A. R., Hopkins P. F., Kim J.-h., Faucher-Giguère C.-A., Keres D., Quataert E., 2016, ApJ, 827, L23
Wilcots E. M., Prescott M. K. M., 2004, AJ, 127, 1900
Wyithe J. S. B., Loeb A., 2006, Nature, 441, 322
Zepf S. E., Koo D. C., 1989, ApJ, 337, 34

APPENDIX A: COMPARISON WITH ILLUSTRIS-DARK-1

Throughout this study we have utilized the *Illustris Hydro* simulation. Here we show that our results are consistent using the dark matter only version of the simulation, *Illustris-Dark-1*.

We follow the same methodology as outlined in Section 2.2.1 to assign a stellar mass to each subhalo in the simulation. The number density of isolated mock dwarfs in *Illustris-Dark-1* is $n_{\rm dwarfiso} = 0.0056 \pm 0.0008$, in good agreement with *Illustris Hydro* (see Table 2).

In the left-hand panel of Fig. A1, we plot the mean number of companions per dwarf per stellar mass bin ($N_{c,m}$) for the *SDSS* catalogue, *Illustris Hydro Projected* catalogue, and its dark matter only counterpart, marked as *Illustris Dark Projected*. This figure is comparable to Fig. 7. Note that the dwarf multiples are selected using only the *Projected* selection criteria of Section 4.1.1. The mock catalogues agree within 1σ, but the *Illustris Dark Projected* results are consistently higher. The average N_c for the entire sample of multiples in *Illustris Dark Projected* is $N_c = 0.040 \pm 0.005$, in good agreement with the *Illustris Hydro Projected* catalogue (Table 3). Results for multiples selected using the *Physical* selection criteria show similar agreement.

The right-hand panel of Fig. A1 shows the "Major Pair" fraction per Primary stellar mass bin for the same catalogues. Again, results agree within 1σ and both mock catalogues exhibits the same behaviour as a function of stellar mass. We conclude that the results presented in this study using *Illustris Hydro* are robust to baryonic effects, which might destroy subhaloes or change their kinematics.

Downloaded from https://academic.oup.com/mnras/article-abstract/480/3/3376/5063581 by California Institute of Technology user on 28 November 2018

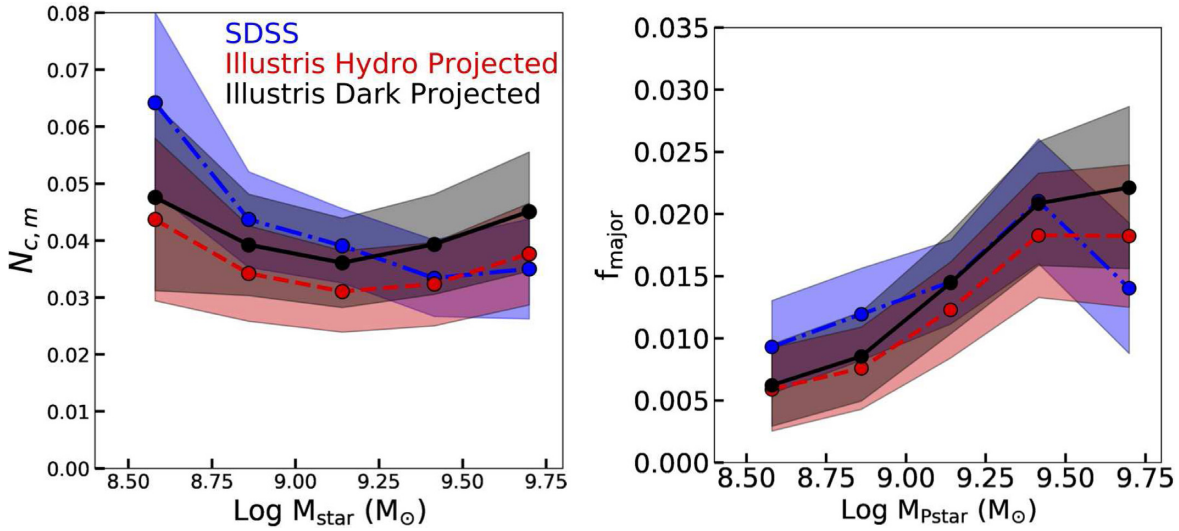

Figure A1. *Left:* The mean number of companions is plotted per stellar mass bin, $N_{c,m}$. This figure is comparable to Fig. 7. *Right:* The fraction of Primary dwarf galaxies that have a Secondary with a stellar mass ratio of $M_{S,star}/M_{P,star} > 1/4$ ("Major Pairs") per Primary stellar mass bin (f_{major}). This is comparable to Fig. 14. In both panels, mock multiples are selected using the *Projected* criteria in the *Illustris Hydro* catalogue (red, dashed) and *Illustris-Dark-1* catalogue (black, solid line). The *SDSS* results are plotted in blue (dash–dotted). Results for both $N_{c,m}$, and f_{major} using the *Illustris Dark Projected* catalogue are consistently higher than that for *Illustris Hydro Projected*, but do agree within 1σ (shaded regions) and exhibit the same behaviour as a function of mass.

This paper has been typeset from a TEX/LATEX file prepared by the author.

Downloaded from https://academic.oup.com/mnras/article-abstract/480/3/3376/5063581 by California Institute of Technology user on 28 November 2018